

## Journal Pre-proofs

Synthesis of 2,3-dihydrobenzo[*b*][1,4]dioxine-5-carboxamide and 3-oxo-3,4-dihydrobenzo[*b*][1,4]oxazine-8-carboxamide derivatives as PARP1 inhibitors

Xuwei Shao, Steven Pak, Uday Kiran Velagapudi, Shruthi Gobbooru, Sai Shilpa Kommaraju, Woon-Kai Low, Gopal Subramaniam, Sanjai Kumar Pathak, Tanaji T. Talele

PII: S0045-2068(20)31372-9  
DOI: <https://doi.org/10.1016/j.bioorg.2020.104075>  
Reference: YBIOO 104075

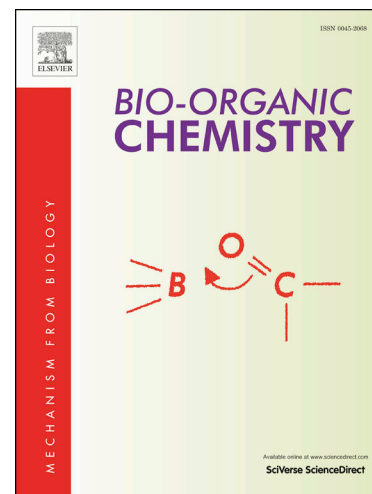
To appear in: *Bioorganic Chemistry*

Received Date: 17 January 2020  
Revised Date: 29 June 2020  
Accepted Date: 3 July 2020

Please cite this article as: X. Shao, S. Pak, U. Kiran Velagapudi, S. Gobbooru, S. Shilpa Kommaraju, W-K. Low, G. Subramaniam, S. Kumar Pathak, T.T. Talele, Synthesis of 2,3-dihydrobenzo[*b*][1,4]dioxine-5-carboxamide and 3-oxo-3,4-dihydrobenzo[*b*][1,4]oxazine-8-carboxamide derivatives as PARP1 inhibitors, *Bioorganic Chemistry* (2020), doi: <https://doi.org/10.1016/j.bioorg.2020.104075>

This is a PDF file of an article that has undergone enhancements after acceptance, such as the addition of a cover page and metadata, and formatting for readability, but it is not yet the definitive version of record. This version will undergo additional copyediting, typesetting and review before it is published in its final form, but we are providing this version to give early visibility of the article. Please note that, during the production process, errors may be discovered which could affect the content, and all legal disclaimers that apply to the journal pertain.

© 2020 Published by Elsevier Inc.



# Synthesis of 2,3-dihydrobenzo[*b*][1,4]dioxine-5-carboxamide and 3-oxo-3,4-dihydrobenzo[*b*][1,4]oxazine-8-carboxamide derivatives as PARP1 inhibitors

Xuwei Shao<sup>a,1</sup>, Steven Pak<sup>a,1</sup>, Uday Kiran Velagapudi<sup>a,1,2</sup>, Shruthi Gobbooru<sup>a</sup>, Sai Shilpa Kommaraju<sup>a</sup>, Woon-Kai Low<sup>a</sup>, Gopal Subramaniam<sup>b</sup>, Sanjai Kumar Pathak<sup>b,c,\*</sup>, Tanaji T. Talele<sup>a,\*</sup>

<sup>a</sup>*Department of Pharmaceutical Sciences, College of Pharmacy and Health Sciences, St. John's University, 8000 Utopia Parkway, Queens, NY 11439, USA*

<sup>b</sup>*Chemistry and Biochemistry Department, Queens College of the City University of New York, 65-30 Kissena Blvd., Flushing, NY 11367, USA;*

<sup>c</sup>*Chemistry Doctoral Program, Biochemistry Doctoral Program, The Graduate Center of the City University of New York, 365 5th Ave, New York, NY 10016, USA*

\* Corresponding authors: E-mail address: [talelet@stjohns.edu](mailto:talelet@stjohns.edu), Tel.: +1 718 990 5405; Fax: +1 718 990 1877; [Sanjai.Kumar@qc.cuny.edu](mailto:Sanjai.Kumar@qc.cuny.edu), Tel.: +1 718 997 4120, Fax: +1 718 997 5531

<sup>1</sup>Authors contributed equally to the work.

<sup>2</sup>Present Address: PACE Analytical Life Sciences, LLC, Suite 102, 19 Presidential Way, Woburn, MA 01801 (U.K.V.).

**Abstract:** Poly(ADP-ribose)polymerase 1 (PARP1), a widely explored anticancer drug target, plays an important role in single-strand DNA break repair processes. High-throughput virtual screening (HTVS) of the Maybridge small molecule library using the PARP1-benzimidazole-4-carboxamide crystal structure and pharmacophore model led to the identification of eleven compounds. These compounds were evaluated using recombinant PARP1 enzyme assay that resulted in the acquisition of three PARP1 inhibitors: **3** (IC<sub>50</sub> = 12 μM), **4** (IC<sub>50</sub> = 5.8 μM), and **10** (IC<sub>50</sub> = 0.88 μM). Compound **4** (2,3-dihydro-1,4-benzodioxine-5-carboxamide) was selected as a lead and it was subjected to further chemical modifications, involving analogue synthesis and scaffold hopping. These efforts led to the identification of (*Z*)-2-(4-hydroxybenzylidene)-3-

oxo-3,4-dihydro-2*H*-benzo[*b*][1,4]oxazine-8-carboxamide (**49**,  $IC_{50} = 0.082 \mu\text{M}$ ) as the most potent inhibitor of PARP1 from the series.

*Keywords:* virtual screening, 1,4-benzodioxine, 1,4-benzoxazin-3-one, PARP1, Knoevenagel condensation

## Introduction

Poly(ADP-ribose) polymerase 1 (PARP1) is the most abundant ( $\sim 10^6$  molecules/cell) member of the PARP family of proteins. It is a chromatin-bound nuclear protein known to facilitate DNA repair processes by catalyzing the poly(ADP)ribosylation (PARylation) of itself (automodification) or on an array of DNA damage repair-associated target proteins (heteromodification) such as topoisomerase I/II, p53, histones, DNA polymerases and DNA ligases [1]. Activation of PARP1 plays a critical role in mediating DNA single-strand break repair in cancer cells, thereby providing them survival advantages. PARP1 inhibitors are therefore being considered clinically as potentiators of chemo- and radio-therapy through suppression of the base excision repair (BER) pathway [2,3]. In addition, some of the FDA approved PARP1 inhibitors (*e.g.*, olaparib, niraparib, rucaparib and talazoparib) exhibited single-agent cytotoxic effect on tumors with germline mutations in *BRCA1*- or *BRCA2*-dependent DNA double-stranded repair mechanisms (homologous recombination, HR) [4,5]. However, the rapid emergence of restored HR pathway function has led to the limited use of existing PARP1 inhibitors [6-8]. Thus, development of new classes of PARP1 inhibitors is highly desirable, and is considered a promising strategy for anticancer drug development.

In our continuing effort to identify novel PARP1 inhibitors [9,10], we conducted a structure- and pharmacophore-based virtual screening of a Maybridge database comprised of a

refined 15,621 small molecule compound library; this initial refinement of the library was generated by applying six pre-defined filtering parameters (Figure 1) to the original 54,836 compound library. Among the 868 virtual hits identified this way, 11 were selected as potential inhibitors of PARP1 enzyme by consideration of novelty, diversity, and lead optimization potential. Further *in vitro* evaluation of these compounds in PARP1 enzyme assay led to the identification of three lead compounds **3** ( $IC_{50} = 12 \mu M$ ), **4** ( $IC_{50} = 5.8 \mu M$ ), and **10** ( $IC_{50} = 0.88 \mu M$ ). Since compound **3** had the weakest PARP1 inhibition and compound **10** belonged to the phthalazinone scaffold, already present in clinically used PARP-inhibitors (e.g., olaparib and talazoparib), we selected 2,3-dihydrobenzo[*b*][1,4]dioxine-5-carboxamide (compound **4**, Figure 1) as a tractable lead for further SAR optimization. Using analogue synthesis and scaffold hopping strategies on compound **4**, we obtained a modestly potent compound **49**, (*Z*)-2-(4-hydroxybenzylidene)-3-oxo-3,4-dihydro-2*H*-benzo[*b*][1,4]oxazine-8-carboxamide ( $IC_{50} = 0.082 \mu M$ , Figure 1) that exhibited a high potential as a lead compound in future anticancer drug development studies targeting PARP1 enzyme.

## Results and Discussion

### Structure-based Virtual Screening

Initially, 54,836 compounds from Maybridge library were subjected to a ligand preparation protocol using six pre-defined parameters such as inclusion of molecular weight filter, controlling ionization, exclusion of tautomers, restricting stereoisomers to one per ligand, number of aromatic rings (1-3) and that all ligands must possess a primary or secondary carboxamide group as depicted in Figure 1. This generated a refined library of 15,621 compounds. These compounds were subsequently subjected to a high-throughput virtual screening (HTVS) protocol using the complex of the catalytic domain of human PARP1 enzyme

and the benzimidazole-4-carboxamide ligand (RCSB Protein Data Bank (PDB) ID: 2RCW). The HTVS with Glide v5.5 docking (Schrodinger LLC, New York, NY) involved constraints such as (1) applying a -7.0 Glide score cutoff to eliminate ligands which have a higher Glide score and (2) employing a hydrogen bond constraint to eliminate the ligands which do not interact with the backbone of Gly863. These efforts led to narrowing of the potential PARP1 inhibitory leads to 900 candidates for pharmacophore-based screening.

### **Pharmacophore-based Virtual Screening**

PHASE algorithm [11] was employed to quantitatively correlate the chemical structures of selected known PARP1 inhibitors to their biological activity for generating a valid pharmacophore model. A training set of 23 known PARP1 inhibitors [12] was chosen for this activity, with their experimental  $pIC_{50}$  values ranging from 0.568 to 2.853 and seven compounds were employed as the test set to validate the accuracy of the pharmacophore models (Table S1, supporting information). Compounds with  $pIC_{50}$  values greater than 1.5 were deemed active for the development of pharmacophore models. A pharmacophore site point generation protocol containing the default variant list: acceptor (A), donor (D), hydrophobic (H), negative (N), positive (P), and aromatic ring (R) along with a diversity of conformers for the training set molecules was selected to generate pharmacophore hypothesis models. Four top-scored pharmacophore hypotheses containing a combination of ADR variants were thus generated (Table S2, supporting information), exhibiting comparable scores for survival, site, vector, volume, and number of active sites. Visual inspection led to elimination of pharmacophore models AADRR.1 and ADRRR.5 due to the incorrect orientation of a vector, thereby preventing the models to form a key hydrogen bonding interaction between carboxamide group of mapped ligands and carbonyl oxygen of Gly863 (Figure S1, supporting information). The pharmacophore

models AADRR.2 and ADRRR.7 were then subjected to atom-based 3D QSAR analysis which provided comparable results for the two models (Table S3, supporting information). Further results of overlapping pharmacophore models on an active PARP1 inhibitor revealed that ADRRR.7 could not identify the key intramolecular hydrogen bonding interaction between carboxamide group and the heteroatom located on the adjacent ring of the ligand (Figure S1, supporting information). Therefore, AADRR.2 was selected for further analysis, and the previously obtained 900 ligands were screened against the AADRR.2 pharmacophore model. During this process, all ligands were required to contain at least three (A2, D3 and R9) of the five features of the AADRR.2 model. This step resulted in 868 ligands, from which 11 compounds were selected for empirical testing in biochemical PARP1 enzyme assay based on their ability to form hydrogen bonding interaction between the carboxamide and Gly863/Ser904, novelty, diversity, and the potential for further optimization (Figure 1)[13].

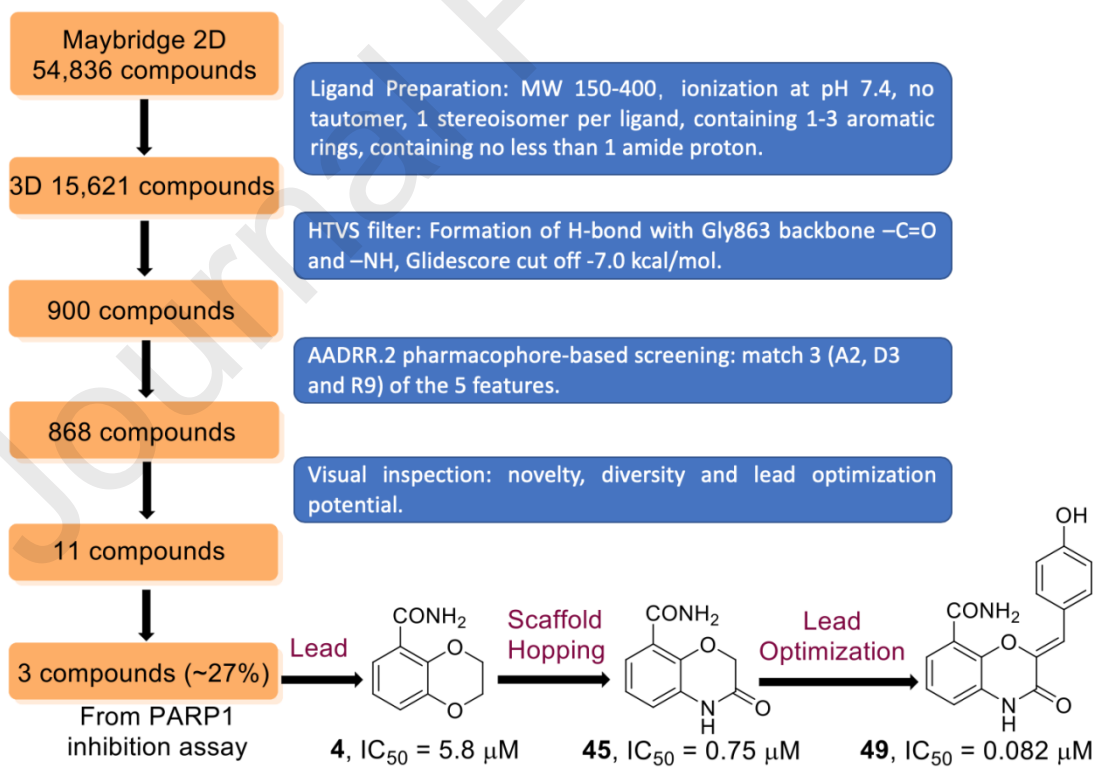


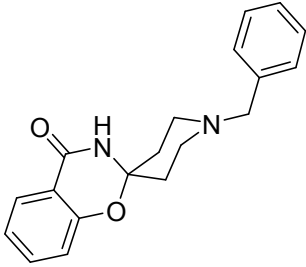
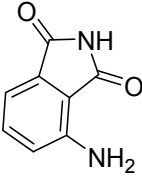
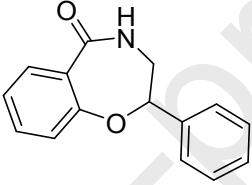
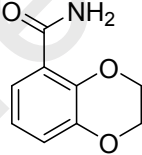
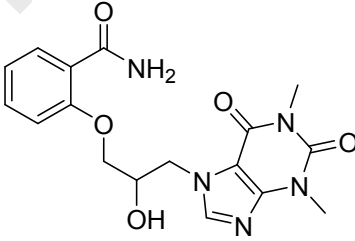
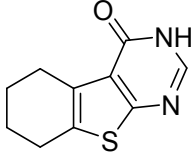
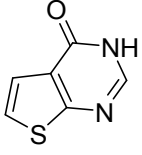
**Figure 1.** A schematic representation of the high-throughput virtual screening protocol and subsequent hit optimization that led to the identification of the most active compound **49**.

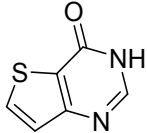
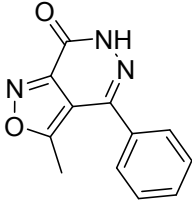
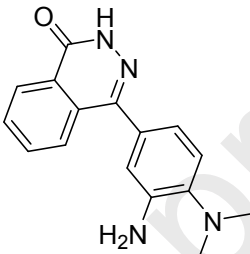
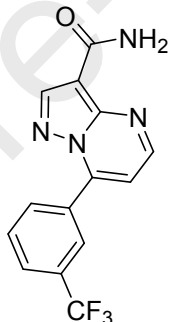
### PARP1 Inhibition Data

Ten of the eleven selected compounds (**1–10**) were obtained from Maybridge Chemicals Ltd (Tintagel, United Kingdom). Compound **11** was purchased from Matrix Scientific (Columbia, SC). These compounds were then tested for *in vitro* inhibition of PARP1 enzyme activity as described in our earlier reports [9,14]. A previously characterized PARP1 inhibitor, 8-amino-2-methylquinazolinone, developed in our laboratory and 3-aminobenzamide, recommended in the assay kit, were included as internal positive controls [14]. The preliminary screening was performed at a single concentration of 10  $\mu\text{M}$  that resulted in three inhibitory classes of compounds: with high, moderate, and low PARP1 inhibitory activity (Table 1). Based on these results, the three best compounds (**3**, **4** and **10**) were selected for further analysis using dose-response relationship. The  $\text{IC}_{50}$  values of these inhibitors thus obtained were 12  $\mu\text{M}$ , 5.8  $\mu\text{M}$  and 0.88  $\mu\text{M}$  for **3**, **4** and **10** respectively (Table 1). Based on the potency and novelty aspects described earlier, compound **4** was selected for further investigation. To that end, the binding model of compound **4** at the active site of PARP1 (Figure S2, supporting information) was generated to facilitate further lead optimization via extension of substituents at the C2- or C3-positions of the dioxine ring or by employing a scaffold hopping strategy.

**Table 1.** Structures and PARP1 inhibitory activities of virtual screening hits **1-11**

Compound	Vendor Number	Structure	PARP1 $\text{IC}_{50}$ ( $\mu\text{M}$ ) <sup>a, b</sup>
----------	---------------	-----------	---

1	S14246		>10
2	AC40100		>10
3	NRB02674 ( <i>R/S</i> )		12 ± 1.6
4	MO00789		5.8 ± 0.10
5	JFD03569 ( <i>R/S</i> )		~10
6	GK03180		~10
7	GK02796		>10

8	GK00357		>10
9	BTB08875		>10
10	BTB02780		0.88 ± 0.090
11	003736		>10

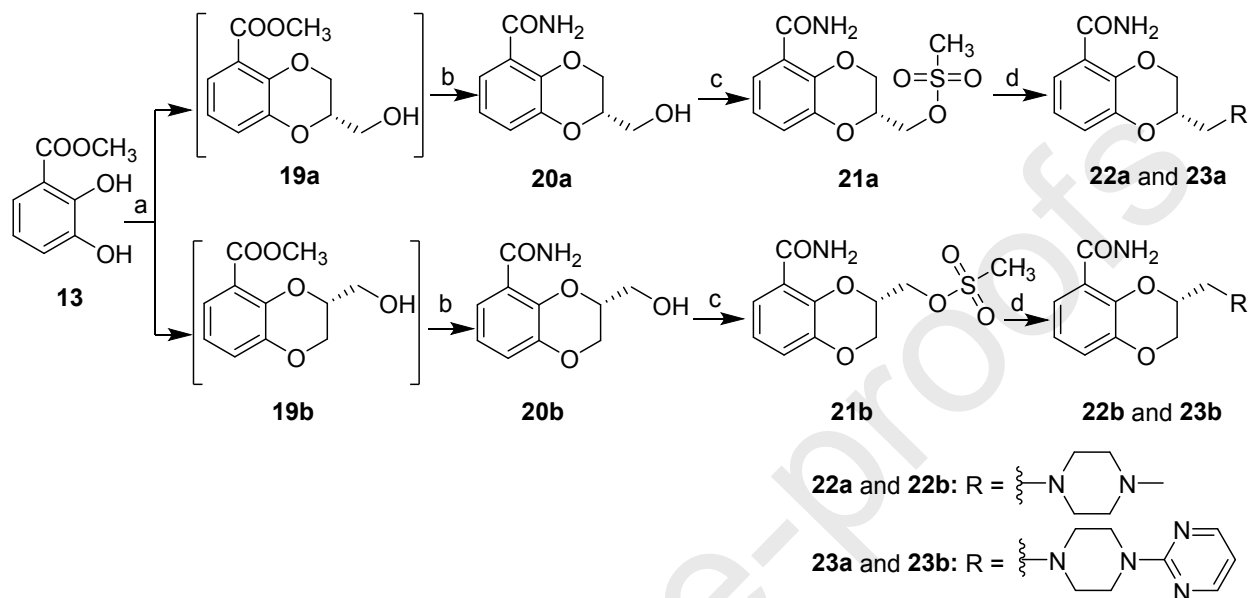
<sup>a</sup>3-Aminobenzamide sample included in the assay kit was used as an internal standard, and showed a consistent result as reported (60 – 80% inhibition at 50  $\mu\text{M}$ ). <sup>b</sup>All compounds were assayed at a single concentration of 10  $\mu\text{M}$  in triplicates. Compounds with <40% inhibition at 10  $\mu\text{M}$  were denoted as PARP1  $\text{IC}_{50}$  >10  $\mu\text{M}$ . Compounds showing 40 – 60% inhibition at 10  $\mu\text{M}$  were considered to have PARP1  $\text{IC}_{50}$  ~10  $\mu\text{M}$ . Compounds showing >60% inhibition at 10  $\mu\text{M}$  were further evaluated to obtain PARP1  $\text{IC}_{50\text{s}}$ .

### Chemistry

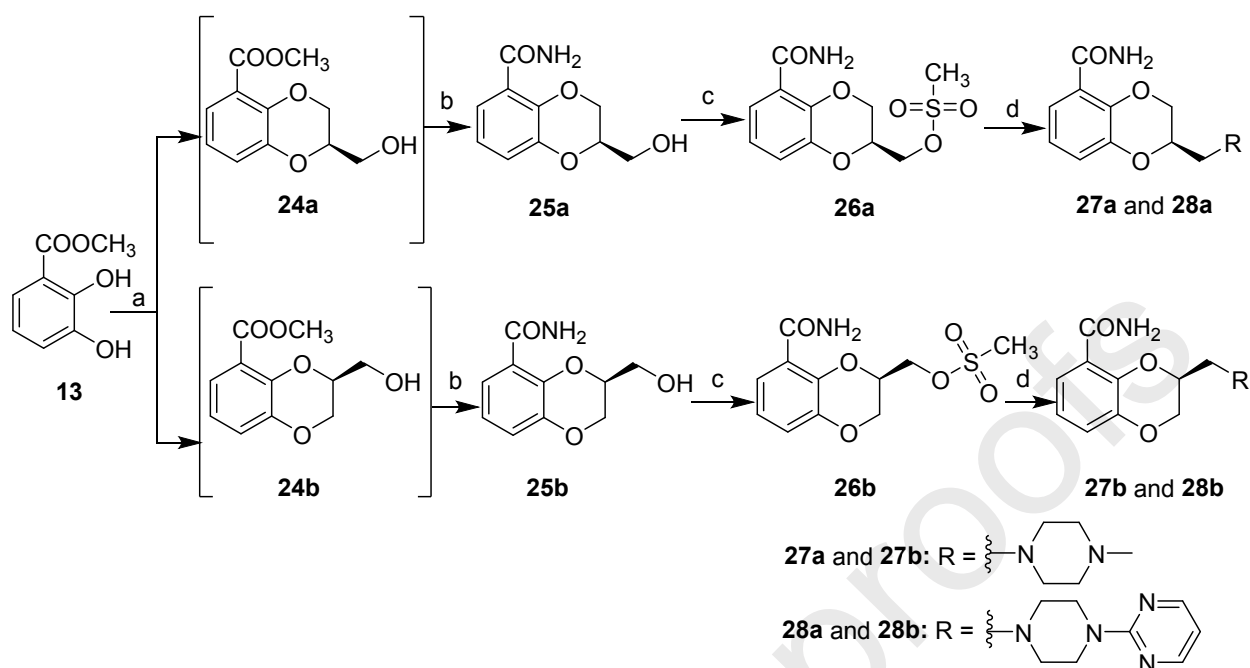
To conduct SAR around compound **4**, it was first synthesized according to Scheme 1. The 2,3-dihydroxybenzoic acid **12** was esterified using concentrated sulfuric acid in refluxing methanol to obtain **13**. Methyl ester **13** was alkylated with 1,2-dibromoethane in the presence of



and **26a/26b** by *N*-methylpiperazine or pyrimidinyl-piperazine yielded **22a/22b**, **23a/23b**, **27a/27b**, and **28a/28b** as shown in Schemes 2 and 3.

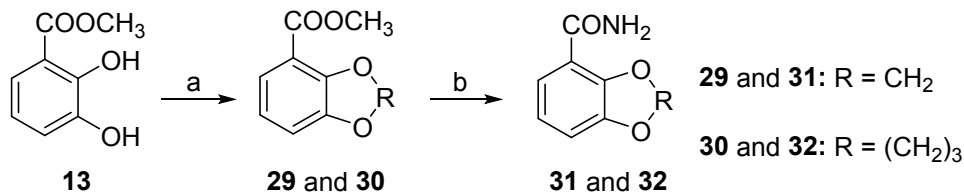


**Scheme 2.** (a) (2*S*)-glycidyl tosylate,  $K_2CO_3$ , DMF, 40 °C, 30 h, 20-30%; (b) (i) LiOH,  $H_2O$ , THF, rt, 10 h; (ii) isobutyl chloroformate, *N*-methylmorpholine, THF, 0 °C, 15-25 min; (iii)  $NH_3$  in MeOH, rt, 1 h, 60-70%; (c) methanesulfonyl chloride, triethylamine, DCM, rt, 10-12 h, 50-55%, (d) *N*-methylpiperazine (for **22a** and **22b**), 1-(2-pyrimidinyl)piperazine (for **23a** and **23b**),  $K_2CO_3$ , DCM, 0 °C to rt, 6-8 h, 20-33%.



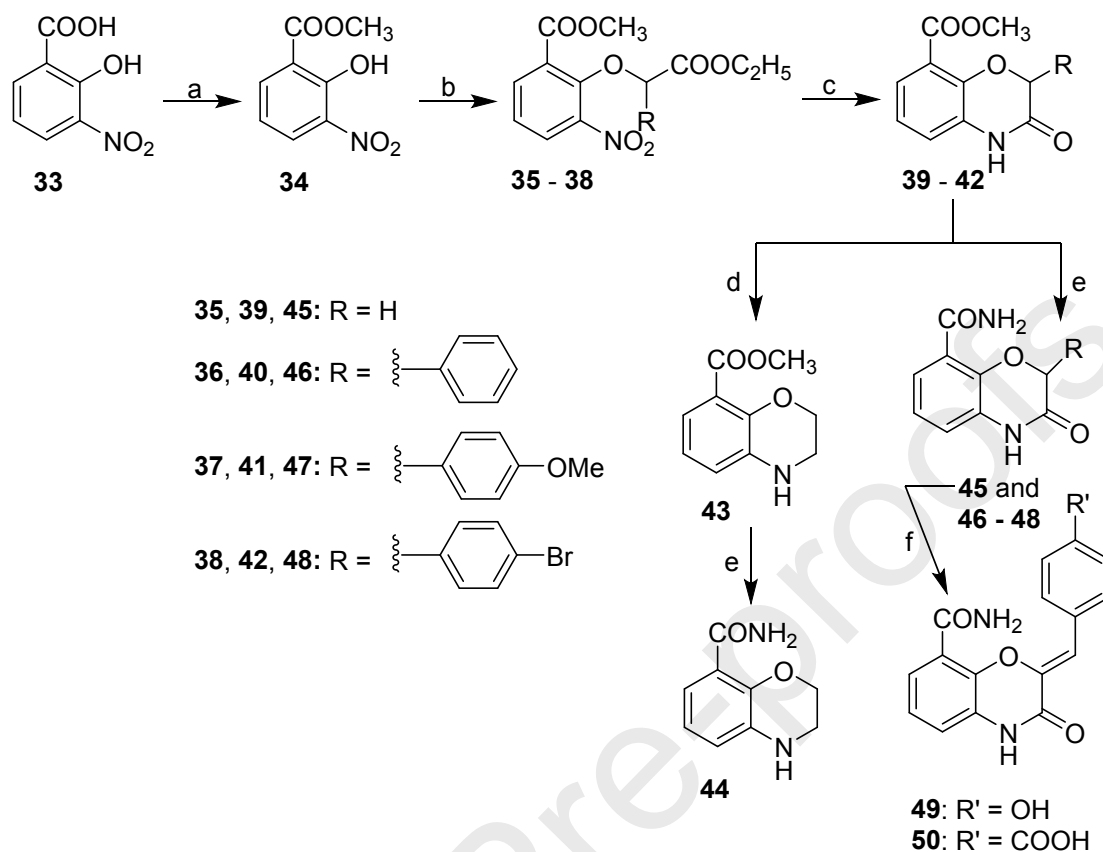
**Scheme 3.** (a) (2*R*)-glycidyl tosylate,  $K_2CO_3$ , DMF, 40 °C, 30 h, 20-30%; (b) (i) LiOH,  $H_2O$ , THF, rt, 10 h; (ii) isobutyl chloroformate, *N*-methylmorpholine, THF, 0 °C, 15-25 min; (iii)  $NH_3$  in MeOH, rt, 1 h, 60-70%; (c) methanesulfonyl chloride, triethylamine, DCM, rt, 10-12 h, 50-55%, (d) *N*-methylpiperazine (for **27a** and **27b**), 1-(2-pyrimidinyl)piperazine (for **28a** and **28b**),  $K_2CO_3$ , DCM, 0 °C to rt, 6-8 h, 18-31%.

With the expectation that scaffold hopping could lead to more potent PARP1 inhibitors, a series of analogues with different core structures were also prepared. Compounds **31** and **32** were first prepared to evaluate the influence of varying dioxine ring size on PARP1 inhibition (Scheme 4). Thus, intermediate **13** was reacted with the dibromomethane or 1,3-dibromopropane, respectively, to obtain **29** and **30** [17]. Esters **29** and **30** were then converted to target carboxamides **31** and **32** following the similar method used for preparing the carboxamide **4** [15].



**Scheme 4.** (a) dibromomethane (for **29**), 1,3-dibromopropane (for **30**), K<sub>2</sub>CO<sub>3</sub>, DMF, reflux, 8-12 h, 55-70%; (b) (i) LiOH, H<sub>2</sub>O, THF, rt, 8-12 h; (ii) corresponding acid, isobutyl chloroformate, *N*-methylmorpholine, THF, 0 °C, 15-30 min; (iii) NH<sub>3</sub> in MeOH, rt, 50-60 min, 60-70%.

To obtain new scaffold hopping analogues, target compounds **44-50** were designed and synthesized by following a synthetic route outlined in Scheme 5. Commercially available acid **33** was initially converted to a methyl ester **34**, and the phenolic hydroxyl group in **34** was subjected to *O*-alkylation with appropriate ethyl  $\alpha$ -bromoacetate that afforded diesters **35-38** [18]. Reductive cyclization of **35-38** with iron and acetic acid afforded intermediates **39-42**. The cyclic amide group in ester **39** was reduced to **43** using NaBH<sub>4</sub> in the presence of boron trifluoride-diethyl etherate complex [19]. Target compounds **44-48** were synthesized according to the procedure used for the synthesis of **4**. Finally, target compounds **49** and **50** were prepared via Knoevenagel condensation reaction conditions using **45** and corresponding benzaldehydes. It is noted that the Knoevenagel condensation reaction produced **49** and **50** in <10% yields. This is attributed to the weak acidic nature of the C2-methylene protons. To increase the amount of product formation, we conducted the reaction using following modifications: (a) conventional reflux of starting reagents in pyridine containing catalytic amounts of the piperidine, (b) microwave irradiation at 120 °C in a 1:1 ratio of acetic anhydride and triethylamine, and (c) microwave irradiation at 120 °C in pyridine containing catalytic amounts of the piperidine. However, the modified conditions did not result in improved product yields.



**Scheme 5.** (a) MeOH, conc. H<sub>2</sub>SO<sub>4</sub>, reflux, 12 h, 88%; (b) appropriate ethyl  $\alpha$ -bromoacetate, K<sub>2</sub>CO<sub>3</sub>, DMF, rt, 8 h, 69-84%; (c) Fe, acetic acid, reflux, 4 h, 69-78%; (d) BF<sub>3</sub>-Et<sub>2</sub>O, NaBH<sub>4</sub>, THF, 5 °C, 2 h, 23%; (e) (i) LiOH, H<sub>2</sub>O, THF, rt, 10 h; (ii) isobutyl chloroformate, *N*-methylmorpholine, THF, 0 °C, 20 min; (iii) NH<sub>3</sub> in MeOH, rt, 30 min, 30-60%; (f) **45**, 4-hydroxybenzaldehyde (for **49**), 4-carboxybenzaldehyde (for **50**), Et<sub>3</sub>N/Ac<sub>2</sub>O (1/1), reflux, 12 h, 8-10%.

### Structural Elucidation of Regioisomers 21a and 21b by HMBC Experiments

Regioisomerism assignments were performed based on the NMR analyses of compounds **21b** and **21a**, as illustrated in Figures 2 and 3 respectively. While 1-bond <sup>1</sup>H-<sup>13</sup>C heteronuclear single quantum coherence (HSQC) spectrum showed similar patterns for the two regioisomers

(Figures S4 and S5, supporting information), the 3-bond long range  $^1\text{H}$ - $^{13}\text{C}$  coupling experiment (HMBC = Heteronuclear Multiple Bond Correlation) not only allowed for assignment of quaternary carbons, but also showed the differences between the two regioisomers. In the 1D proton spectrum H6 and H4 appear as doublets whereas H5 appears as a triplet. Assignment of H6 was confirmed by the 3-bond coupling to the carbonyl carbon in the HMBC spectra (peak C in Figures 2 and 3). Identifying H6 allowed for the identification of quaternary carbon, C2 (peak B in Figures 2 and 3) through its 3-bond coupling, while quaternary carbon, C3 was identified by its 3-bond coupling to H5 (peak E in Figures 2 and 3). Unequivocal assignment of C2 and C3 was utilized to find if C8 or C9 were substituted with a functional group. In the expanded HMBC spectra of **21b** shown in Figure 2, C3 showed 3-bond coupling to a pair of methylene protons (peaks F and G). This was possible only if there was no substituent on C9. On the other hand, in the expanded HMBC spectra of **21a** shown in Figure 3, C2 showed 3-bond coupling to a pair of methylene protons (peaks F and G) clearly indicating that C8 was unsubstituted. The regiochemistry of the hydroxymethyl, *N*-methylpiperazine and pyrimidinyl-piperazine substituted compounds was also assigned based on the fact that they shared the same intermediates such as **19a/19b** and **24a/24b**.

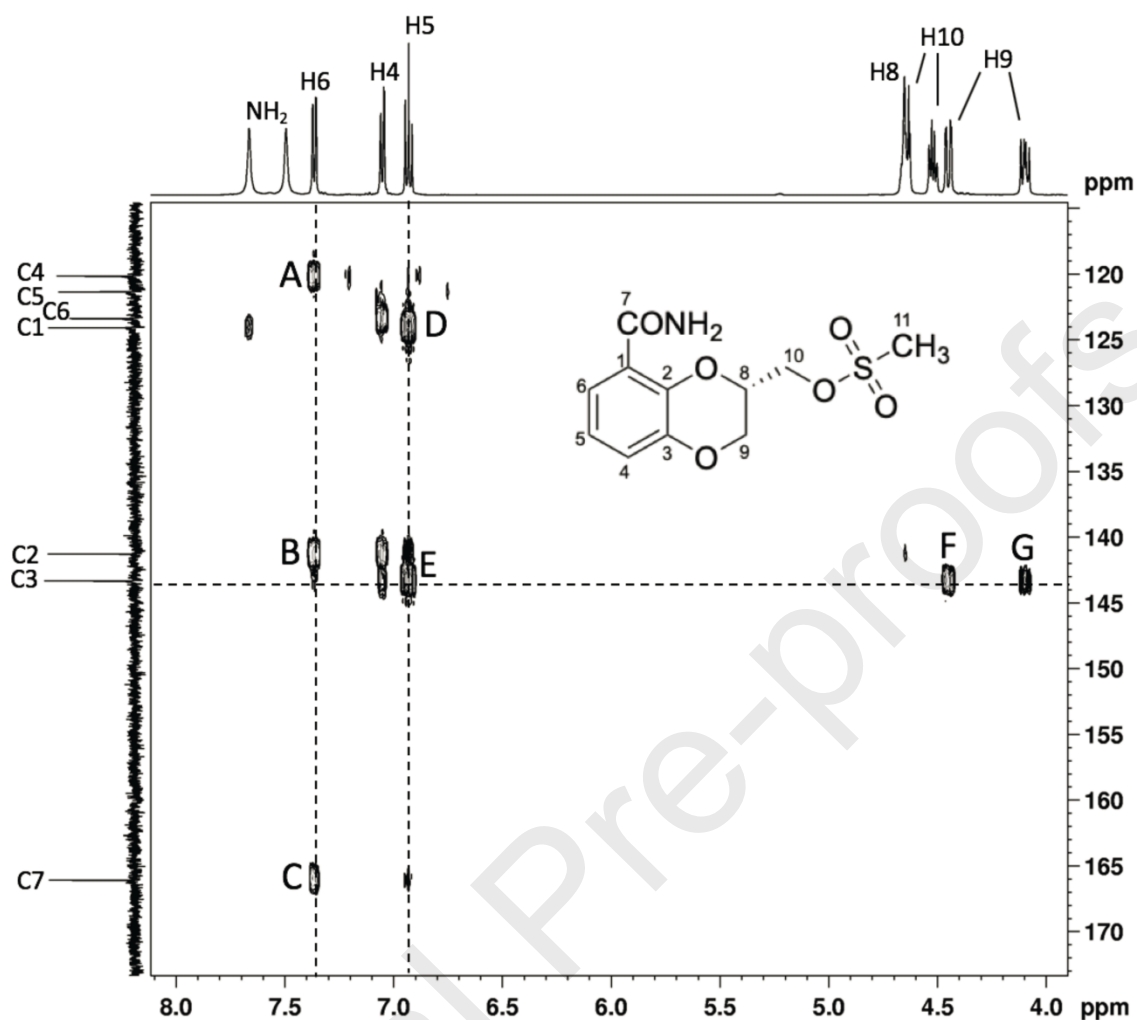


**Figure 2.**  $^1\text{H}$ - $^{13}\text{C}$  HMBC spectra of **21b** regioisomer: Crosspeaks identified as A, B, and C are 3-bond couplings from H6 to C4, C2, and C7 respectively. Crosspeaks identified as D and E are 3-bond couplings from H5 to C1 and C3. Crosspeaks identified as F and G are 3-bond couplings from the C9 methylene protons to C3 confirming that the C9 carbon is unsubstituted.

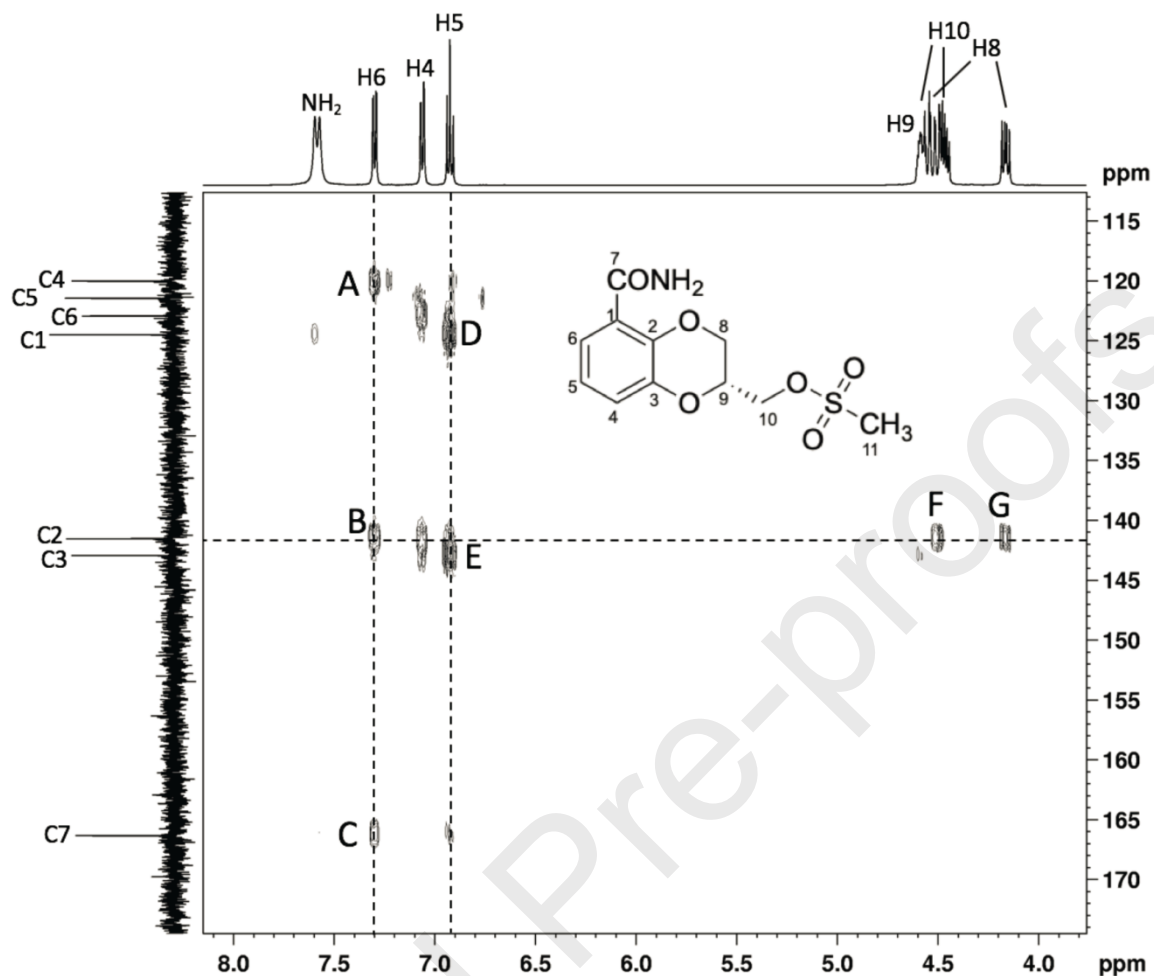


**Figure 3.**  $^1\text{H}$ - $^{13}\text{C}$  HMBC spectra of **21a** regioisomer: Crosspeaks identified as A, B, and C are 3-bond couplings from H6 to C4, C2, and C7 respectively. Crosspeaks identified as D and E are 3-bond couplings from H5 to C1 and C3. Crosspeaks identified as F and G are 3-bond couplings from the C8 methylene protons to C2 confirming that the C8 carbon is unsubstituted.

### Structure-Activity Relationship

Initial structure- and pharmacophore-based virtual screening studies led to the identification of 11 compounds that were categorized into three classes: with high, moderate, or low PARP1 inhibition (Table 1). Based on novelty of structure and ease of synthesis, we selected compound **4** ( $\text{IC}_{50} = 5.8 \mu\text{M}$ ) as our lead for further optimization. PARP-inhibitory positive

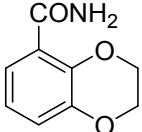
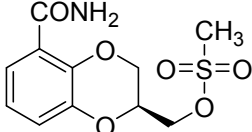
controls (olaparib and veliparib) were used for comparison. Table 2 summarizes the installation of small to large substitutions at various positions on the bicyclic ring system of **4** and their resulting effects on activities. To obtain a direct comparison of activities between optimized analogues and lead compound **4**, percentage inhibition against PARP1 by target compounds at 5  $\mu\text{M}$  was determined. The compounds showing >60% inhibition were evaluated for their  $\text{IC}_{50}$  values. Introduction of nitro (**15** and **16**) or amino (**17** and **18**) groups on the phenyl portion of the benzodioxine ring led to a dramatic loss of activity. Further we wanted to explore the effect of various polar substituents on the dioxine portion of lead compound **4**. Synthesis of compounds with such substitutions will generate a stereogenic center for each modification. To avoid the complexity involved in the purification and identification of active enantiomers, a synthetic route that would simplify both chemistry and SAR interpretation was necessary. As a result, we optimized the synthesis using two homochiral glycidyl tosylates as the starting materials. This assisted us in achieving the synthesis of the pure enantiomers with a desirable purity and additionally, the synthesis gave rise to two regioisomers for each enantiomer. The compound library thus generated, comprising **20a-23a**, **20b-23b**, **25a-28a**, and **25b-28b**, was screened *in vitro* against PARP1 enzyme (see Table 2).

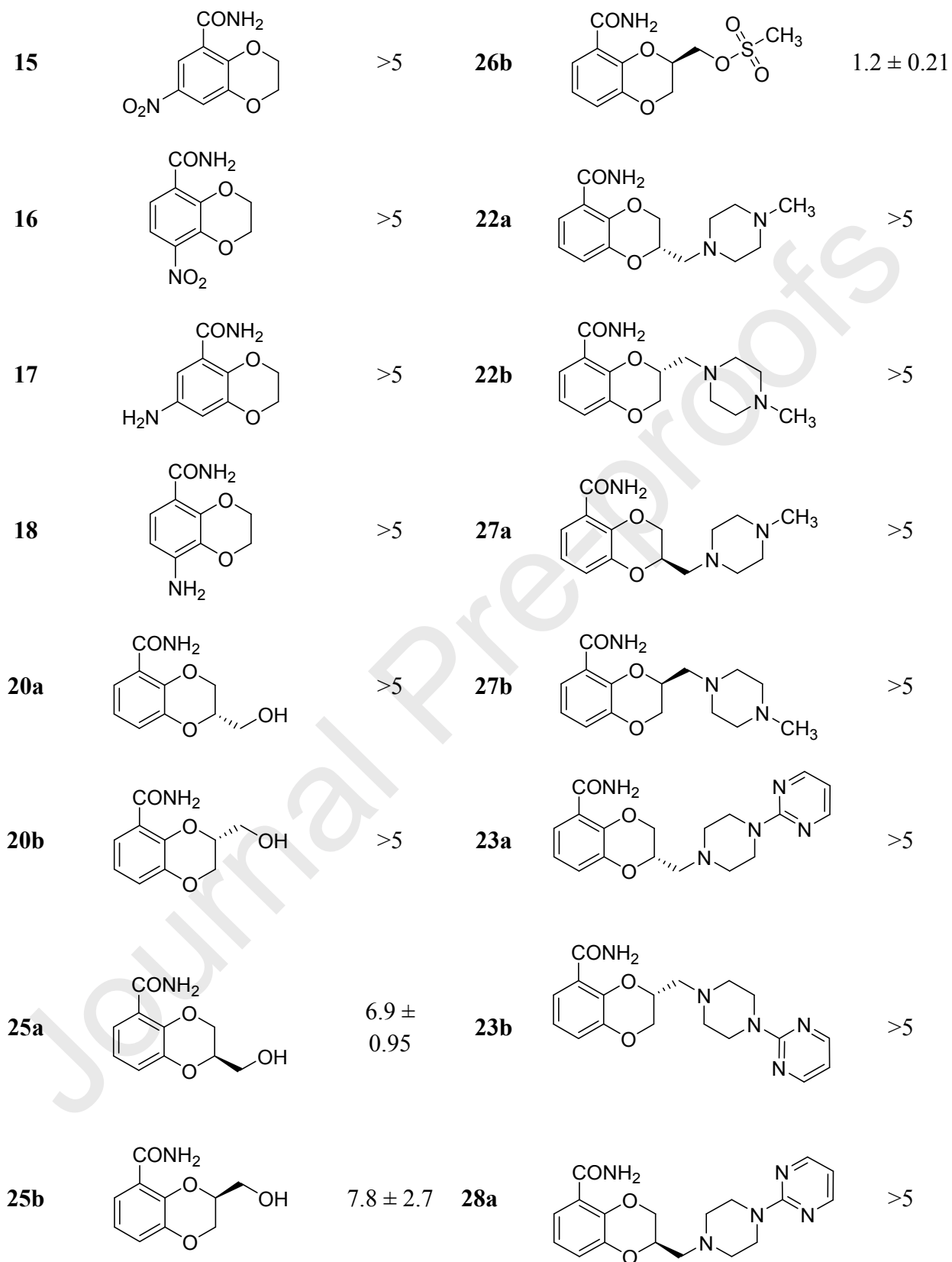
While analogues with hydroxymethyl extension, **25a** (with C2-substitution,  $\text{IC}_{50} = 6.9 \mu\text{M}$ ) and **25b** (with C3-substitution,  $\text{IC}_{50} = 7.8 \mu\text{M}$ ) displayed comparable activities as that of lead compound **4**, the modifications leading to compounds **20a** and **20b** proved detrimental. Enantiomerically pure hydroxymethyl regioisomers were then converted to respective methanesulfonates **21a**, **21b**, **26a** and **26b** with the hypothesis that they would capture additional hydrogen bonding interactions in the adenosine-binding pocket (ABP) of PARP1 active site. Interestingly, C3-substituted enantiomers **21b** ( $\text{IC}_{50} = 0.69 \mu\text{M}$ ) and **26b** ( $\text{IC}_{50} = 1.2 \mu\text{M}$ )

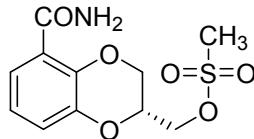
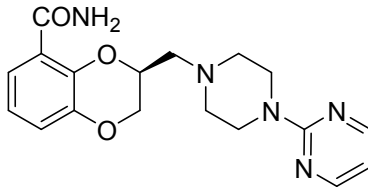
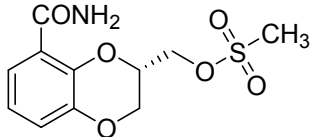
exhibited ~8-fold and ~5-fold improvement in activity, compared to the unsubstituted lead **4** ( $IC_{50} = 5.8 \mu M$ ), while analogues **21a** and **26a** with C2-mesylate demonstrated a loss of PARP1 inhibition. Compound **21b** also showed ~10-fold improved activity over hydroxymethyl precursor **25a**. From these results, it was evident that methanesulfonyl extensions at the C3-position were more favored regardless of its stereochemistry, compared to those at the C2-position. In conclusion, compound **21b** with (*S*)-configuration was the most potent amongst these four analogues.

To further assess the importance of methanesulfonyl group, we developed a compound library where this group was displaced with *N*-methylpiperazinyl extension resulting in compounds, **22a**, **22b**, **27a**, and **27b** (see Table 2). This modification was anticipated to capture ionic and/or hydrogen bonding interactions within the ABP of PARP1 active site; however, these analogues showed a significant decrease (<20% inhibition at 5  $\mu M$ ) in the activity profile compared to the lead compound **4** ( $IC_{50} = 5.8 \mu M$ ). Furthermore, replacement of the methyl group in *N*-methylpiperazine with a 2-pyrimidinyl extension (analogues **23a**, **23b**, **28a** and **28b**) also exhibited a significant loss of activity (<20% inhibition at 5  $\mu M$ ). These results together suggested that bulky extensions at the C2- or C3-positions, were perhaps pointing toward a sterically hindered region in the active site of PARP1.

**Table 2.** PARP1 inhibitory activities of target compounds **15-18**, **20-23**, and **25-28**

Compd	Structure	PARP1 $IC_{50}$ ( $\mu M$ ) <sup>a,b</sup>	Compd	Structure	PARP1 $IC_{50}$ ( $\mu M$ ) <sup>a,b</sup>
<b>4</b>		5.8 ± 0.10	<b>26a</b>		>5



<b>21a</b>		>5	<b>28b</b>		>5
<b>21b</b>		0.69 ± 0.27			
<b>Ola<sup>c</sup></b>	-	0.0012 ± 0.00020	<b>Veli<sup>d</sup></b>	-	0.0015 ± 0.00020

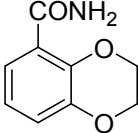
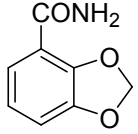
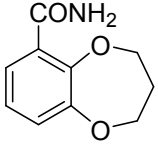
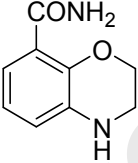
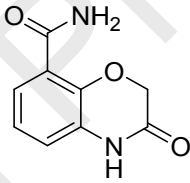
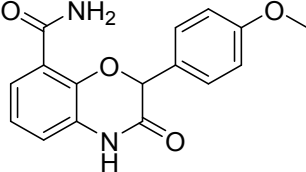
<sup>a</sup>3-Aminobenzamide sample included in the assay kit was used as an internal standard, and showed a consistent result as reported (60 – 80% inhibition at 50  $\mu$ M). <sup>b</sup>All compounds were assayed at a single concentration of 5  $\mu$ M in triplicates. Compounds with <40% inhibition at 5  $\mu$ M were denoted as PARP1 IC<sub>50</sub> >5  $\mu$ M. Compounds showing >60% inhibition at 5  $\mu$ M were further evaluated to obtain PARP1 IC<sub>50</sub>s. <sup>c</sup>olaparib; <sup>d</sup>veliparib

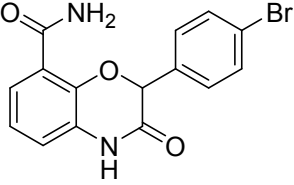
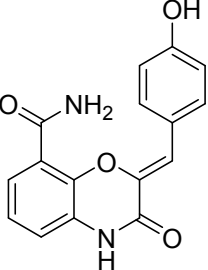
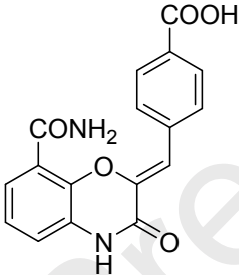
Finally, to further improve the inhibitory potency of benzodioxine lead compound **4**, the scaffold hopping strategy was implemented. We therefore explored the effect of modifying the size of the fused ring system and studied its effect on inhibitory potency (Table 3). With the intention of securing compounds with enhanced potency, target compounds that exhibited >60% inhibition at 2.5  $\mu$ M concentration were prompted for PARP1 IC<sub>50</sub> determination. The synthesized benzodioxole compound **31** exhibited an IC<sub>50</sub> value of  $\geq 2.5$   $\mu$ M (literature IC<sub>50</sub> = 5.3  $\mu$ M [20] while benzodioxepine **32** showed significantly decreased activity (15% inhibition at 2.5  $\mu$ M). This data suggested that the six-membered ring was perhaps the optimum size ring for PARP1 inhibitory activity. To evaluate the contribution of the oxygen atom in the dioxine ring, we replaced one of the oxygen atoms (H-bond acceptor) in compound **4** with bioisosteric –NH– (H-bond donor) group. Our hypothesis, based on structural evidence, was that this modification

could significantly improve PARP1 inhibition through favorable water-mediated hydrogen bonding interaction with the catalytically crucial Glu988 residue in the nicotinamide binding pocket. To our surprise, 1,4-benzoxazine derivative **44** ( $IC_{50} = 11 \mu M$ ) was  $\sim 2$ -fold less potent than **4**. However, converting a moderately basic ring amine in **44** to a neutral cyclic carboxamide led to **45** that exhibited 15-fold enhanced activity ( $IC_{50} = 0.75 \mu M$ ) in comparison to **44**. This improvement in potency may be attributed to a water-mediated hydrogen bonding interaction of **45** with Glu988 residue. Analogue **45** was considered as a refined lead compound and subsequent substitutions were performed at its C2-position to enhance hydrophobic/hydrogen bonding interactions. A phenyl extension at C2-position was thus introduced as a racemate to capture hydrophobic interactions, which resulted in decreased activity (**46**,  $IC_{50} \sim 2.5 \mu M$ ). Electron-donating (methoxy) or electron-withdrawing (bromo) substitutions at the *para*-position of the C2-phenyl led to racemic mixtures **47** (methoxy) and **48** (bromo). Compound **47** ( $IC_{50} = 0.80 \mu M$ ) displayed a comparable activity whereas **48** ( $IC_{50} > 2.5 \mu M$ ) showed decreased activity with respect to **45**. Since benzylidene substitutions in our previously published work proved successful in generating potent analogues, [9,15] we decided to introduce a rigid substitution such as *para*-substituted benzylidene moiety at the C2-position. This led to the synthesis of two compounds with further gain in potency, e.g., compounds **49** ( $IC_{50} = 0.082 \mu M$ ) and **50** ( $IC_{50} = 0.42 \mu M$ ). The pattern in which various structural modifications of the benzodioxine and benzoxazinone scaffolds favor or disfavor PARP1 inhibition is depicted in Figure 4.

**Table 3.** PARP1 inhibitory activities of Scaffold Hopping analogues

Compound	Structure	PARP1 $IC_{50}$ ( $\mu M$ ) <sup>a,b</sup>
----------	-----------	---

4		$5.8 \pm 0.10$
31		$>2.5$ (5.3) <sup>c</sup>
32		$>2.5$
44		$11 \pm 1.9$
45		$0.75 \pm 0.090$
46		$\sim 2.5$
47		$0.80 \pm 0.15$

48		>2.5
49		$0.082 \pm 0.045^d$
50		$0.42 \pm 0.046^d$
Ola <sup>e</sup>	-	$0.0012 \pm 0.00020$
Veli <sup>f</sup>	-	$0.0015 \pm 0.00020$

<sup>a</sup>3-Aminobenzamide sample included in the assay kit was used as an internal standard, and showed a consistent result as reported (60 – 80% inhibition at 50  $\mu\text{M}$ ). <sup>b</sup>All compounds were assayed at a single concentration of 2.5  $\mu\text{M}$  in triplicates. Compounds with <40% inhibition at 2.5  $\mu\text{M}$  were denoted as PARP1  $\text{IC}_{50}$  >2.5  $\mu\text{M}$ . Compounds showing 40 - 60% inhibition at 2.5  $\mu\text{M}$  were considered to have PARP1  $\text{IC}_{50}$  ~2.5  $\mu\text{M}$ . Compounds showing >60% inhibition at 2.5  $\mu\text{M}$  were further evaluated to obtain PARP1  $\text{IC}_{50}$ . <sup>e</sup>Literature  $\text{IC}_{50}$  value; <sup>d</sup>Upon observing >70% inhibition at 0.5  $\mu\text{M}$  in PARP1 enzyme assay,  $\text{IC}_{50}$  values of compounds **49**, **50**, olaparib, and

veliparib were determined by chemiluminescence assay (BPS Bioscience, San Diego, CA);  
<sup>e</sup>olaparib; <sup>f</sup>veliparib

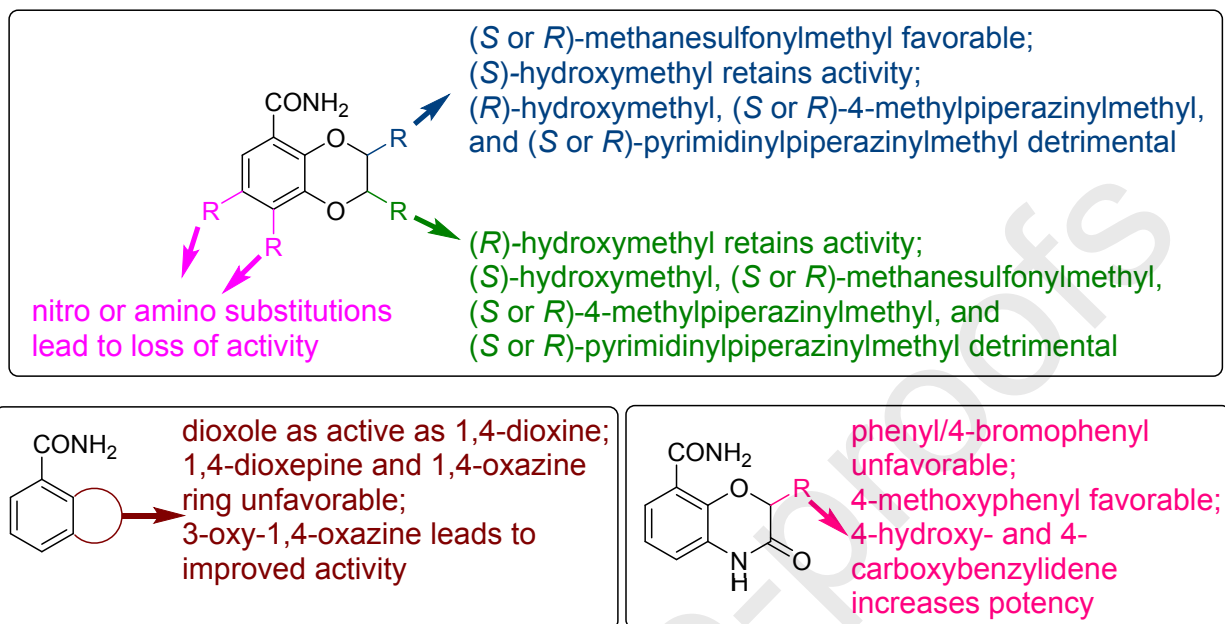


**Figure 4.** SAR summary of the 1,4-benzodioxine and 3-oxo-2,3-dihydrobenzoxazine scaffolds.

Because PARP-isoform selectivity is a key to obtain clinically useful new compounds to treat cancers, we conducted screening of the most potent compound **49** along with positive controls against seven clinically investigated PARP-isoforms (e.g., PARP2, PARP3, TNKS1 (PARP5A), TNKS2 (PARP5B), PARP8, PARP10, and PARP14 (Figure 5 and Table S5). Compound **49** (PARP1  $IC_{50} = 0.082 \mu\text{M}$ ) showed complete inhibition of PARP2 at  $0.5 \mu\text{M}$  concentration, which is not surprising due to a highly conserved catalytic domain (>69% homology) being shared by both PARP1 and PARP2.[21] Interestingly, **49** also substantially inhibited PARP3, TNKS1, and TNKS2, which are involved in cancer progression.[22,23] Conversely, **49** did not interfere with other PARP-isoforms such as PARP8, PARP10 or PARP14. Further investigation on PARP-isoform screening with low testing concentrations will be conducted based on the progress of future structure optimization.

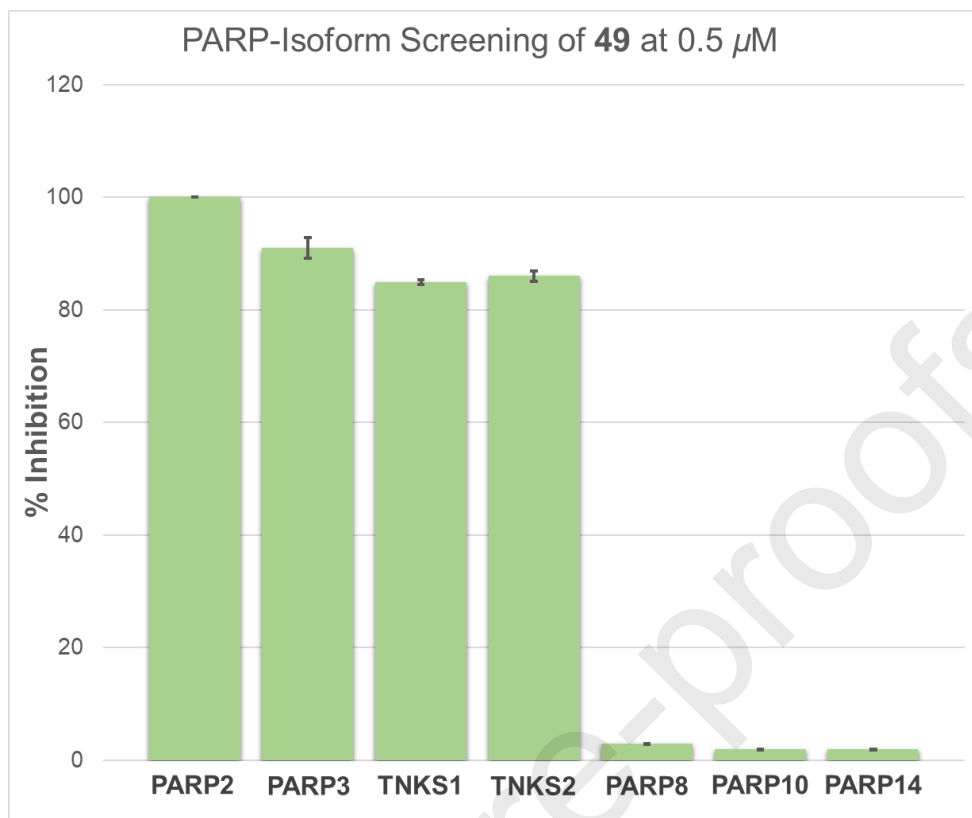


**Figure 5. Percentage inhibition data of 49 against seven PARP-isoforms.** The reported data is based on the two independent experiments, and each experiment was performed in duplicate. **Olaparib** for PARP2, PARP3, PARP8, and PARP10, **XAV- 939** for TNKS1 and TNKS2 and **rucaparib** for PARP14 were used as the positive controls (%inhibition data of the positive controls are reported in supporting information, Table S5).

To elucidate the plausible binding interactions of the most potent compound **49** at the active site of PARP1, we docked compound **49** using the Glide docking tool and co-crystal structure of full length PARP1-dihydrobenzofuran-7-carboxamide (Figure 6) [15]. In the binding model, the pharmacophore carboxamide group of **49** captures three key hydrogen bonding interactions with the side chain of Ser904 and the backbone atoms of Gly863, similar to what we observed for lead **4** (Figure S2, supporting information). Furthermore, a productive

intramolecular hydrogen bond between the amide proton and the oxazinone ring oxygen atom was also evident. The phenyl ring of the benzoxazinone moiety formed a  $\pi$ - $\pi$  stacking interaction with the side chain of Tyr907. The 4-hydroxybenzylidene moiety extended toward the ABP of the PARP1 active site while forming a hydrogen bond with the side chain of Ser864. Additionally, the phenolic hydroxyl group of **49** could form an electrostatic contact with the side chain of a key residue Asn868 due to the proximity between the two groups [9]. The benzoxazinone ring -NH- is found located near Glu988, which suggests a plausible water-mediated hydrogen bonding. Future studies will explore the effect of a wide range of substituents on the benzylidene ring to extend the molecule further into the ABP of PARP1 enzyme. These efforts will be facilitated by optimizing the reaction conditions for the Knoevenagel condensation, which is the low-yielding final step to produce target compounds.

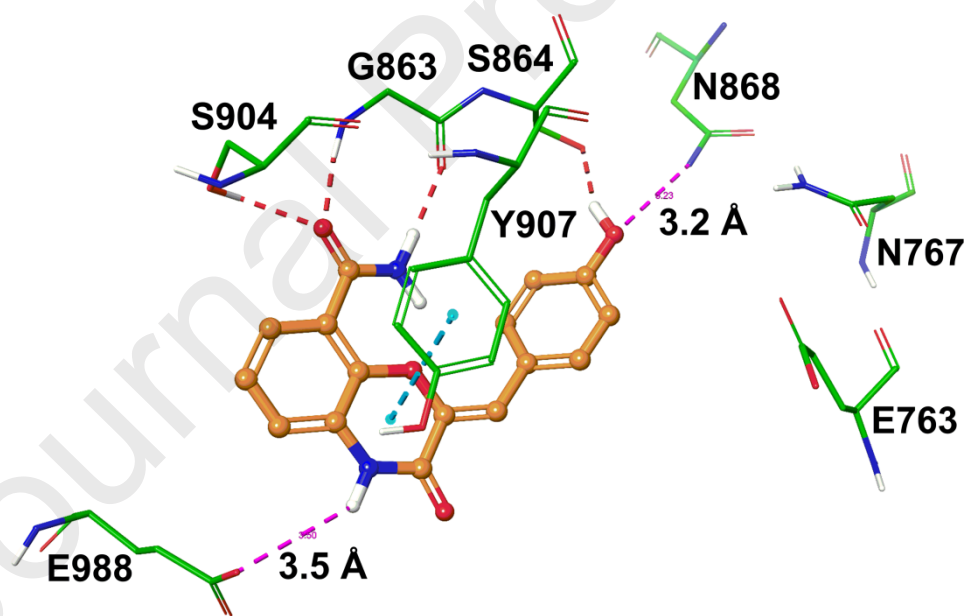


**Figure 6.** A binding model of **49** in the active site of PARP1. Key amino acids are depicted in stick model with the atoms colored as carbon – green, hydrogen – white, nitrogen – blue, and oxygen – red. The ligand is shown in ball and stick model with the same color scheme as above

except carbon atoms are represented in orange. The broken red, pink and cyan lines indicate hydrogen bonding interaction, potential electrostatic contacts and  $\pi$ - $\pi$  interaction, respectively.

## Conclusion

In this study, PARP1 inhibitory hit compound **4** was first identified from a structure- and pharmacophore-based virtual screening protocol. Polar substitutions installed at the C2- or C3-positions of the benzodioxine ring of **4** led to analogues **21b** and **26b** with improved enzymatic inhibitory activities. Finally, utilization of the scaffold hopping strategy identified a refined lead compound **45** that was further optimized to generate a potent PARP1 inhibitor **49**. Binding models of key compounds in the PARP1 active site allowed rationalization of the observed SAR trends. It is anticipated that compound **49** will serve as a promising lead compound for generation of selective PARP1 inhibitory agents with low nanomolar potency.

## Experimental

### High-throughput virtual screening

A detailed information regarding high-throughput virtual screening (ligand preparation, protein refinement, Glide docking procedure, and 3D pharmacophore modeling) can be found in supporting information.

### Materials and methods

The selected 11 compounds from HTVS were obtained from Maybridge Chemicals Ltd. (Tintagel, United Kingdom) and Matrix Scientific (Columbia, SC). Starting materials for synthesis were received from the following vendors and used as received: Aldrich Chemical Co. (Milwaukee, WI), AK scientific (Union City, CA), Combi-Blocks Inc. (San Diego, CA), TCI America (Portland, OR), Gold Biotechnology (St. Louis, MO), Sigma-Aldrich (St. Louis, MO)

and Alfa Aesar (Ward Hill, MA). The uniformity of all synthesized compounds was confirmed by thin layer chromatography (Agela Technologies). Thin layer chromatography (TLC) was employed to monitor the progress of reactions at 254 nm ultraviolet light. Bruker 400 Ultrashield™ spectrometer ( $^1\text{H}$  at 400 MHz and  $^{13}\text{C}$  at 100 MHz) equipped with a z-axis gradient probe was used to record NMR experiments. Tetramethylsilane (TMS) was used as an internal standard, and chemical shift ( $\delta$ ) of  $^1\text{H}$  NMR was reported downfield of the TMS signal in parts per million (ppm). The  $^1\text{H}$  NMR data are presented as follows: chemical shift [multiplicity s (singlet), br (broad singlet), d (doublet), t (triplet), q (quartet), dd (doublet of doublets), and m (multiplet), number of protons, coupling constant]. 2D NMR experiments were carried out on Avance III NMR spectrometer with a  $^1\text{H}$  frequency of 500 MHz and  $^{13}\text{C}$  frequency of 125 MHz and equipped with an inverse probe. Samples were dissolved in DMSO- $d_6$  or chloroform- $d$  and experiments were carried out at room temperature.  $^1\text{H}$  and  $^{13}\text{C}$  chemical shift assignments were carried out with the aid of  $^1\text{H}$ - $^1\text{H}$  COSY,  $^1\text{H}$ - $^{13}\text{C}$  HSQC and  $^1\text{H}$ - $^{13}\text{C}$  HMBC experiments. Purification by flash chromatography was performed on Reveleris X2 flash chromatography system (BUCHI Corporation, New Castle, DE). High resolution mass spectra (HRMS) were collected for all unknown target compounds using a Waters Xevo G2-XS QToF mass spectrometer equipped with H-Class UPLC inlet and a LockSpray ESI source. Chiral HPLC analysis was performed using Agilent 1100 HPLC system and column (250 mm  $\times$  4.00 mm, serial no. 111156). Compounds were dissolved in acetonitrile and injected (10  $\mu\text{L}$ ) into Chirex column (phenomenex, Torrance, CA) with stationary phase as (*S*)-valine and (*R*)-1-( $\alpha$ -naphthyl)ethylamine. Optimum resolution of the enantiomers was achieved using isocratic mobile phases eluting at a flow rate of 1 mL/min. The elution was monitored at UV 254 nm in the form of major and minor peaks representing each enantiomer. Enantiomeric excess (%ee)

was calculated based on the following equation,  $ee = ((R-S)/(R+S)) \times 100\%$ , where (*R*) and (*S*) denote individual optical isomers in the mixture and (*R*) + (*S*) = 1.

## Synthetic procedures

**General procedure to convert ester-containing intermediate to respective amides using mixed-anhydride method (A)** [15]. Mixture of ester containing intermediate (2.0 mmol), lithium hydroxide (0.096 g, 4.0 mmol), and water (2 mL) in 10 mL of tetrahydrofuran was stirred at room temperature for 10 h. After removal of solvent under vacuum, the reaction mixture was diluted with ethyl acetate and extracted with water. The aqueous extract was then acidified using 2N aqueous hydrochloric acid solution followed by extraction with ethyl acetate (3 X 20 mL). The combined organic portion was dried over anhydrous magnesium sulfate, and concentrated under reduced pressure to obtain the corresponding acid, which was subjected to the next step without further purification.

The acid was dissolved in 10 mL tetrahydrofuran, and the temperature was reduced to 0 °C under nitrogen atmosphere. After addition of isobutyl chloroformate (0.3 mL, 2.2 mmol) and *N*-methylmorpholine (0.24 mL, 2.2 mmol), the same condition was maintained until acid was completely converted to the desired mixed anhydride intermediate as monitored by TLC. Then a 2.0 mL solution of 7N ammonia in methanol was added, and the reaction mixture was stirred for 20 min at room temperature. After extraction with ethyl acetate and water, crude product was purified using flash chromatography with appropriate combination of ethyl acetate and hexanes.

**Methyl 2,3-dihydroxybenzoate (13)** [24]. To a solution of 2,3-dihydroxybenzoic acid (0.3 g, 1.9 mmol) in 20 mL of methanol, concentrated sulfuric acid (0.3 mL) was added at 5 °C. The

reaction mixture was refluxed for 12 h, cooled to room temperature, and concentrated under vacuum. The resulted mass was dissolved in ethyl acetate and washed with sodium carbonate solution three times. The organic extract was dried over magnesium sulfate and concentrated under reduced pressure to obtain **13** as a white powder (yield: 0.278 g, 85%). <sup>1</sup>H NMR (400 MHz; DMSO-*d*<sub>6</sub>; TMS) δ 9.94 (s, 2H), 7.23 (dd, *J* = 8.0 Hz, 1.6 Hz, 1H), 7.04 (dd, *J* = 7.9 Hz, 1.6 Hz, 1H), 6.75 (t, *J* = 7.9 Hz, 1H), 3.88 (s, 3H).

**Methyl 2,3-dihydrobenzo[*b*][1,4]dioxine-5-carboxylate (14)** [17]. 1,2-Dibromoethane (0.17 mL, 2.0 mmol) was added to a suspension of **13** (0.336 g, 2.0 mmol) and K<sub>2</sub>CO<sub>3</sub> (0.304 g, 2.2 mmol) in 5 mL dimethylformamide. The reaction mixture was stirred under reflux for 10 h. When the starting material was completely consumed as indicated by TLC, the mixture was diluted with water and extracted with ethyl acetate. The organic portion was dried over anhydrous magnesium sulfate and evaporated under reduced pressure. The crude product was purified by flash chromatography (ethyl acetate:*n*-hexane 10:90) to obtain **14** as a white powder (yield: 0.272 g, 70%). <sup>1</sup>H NMR (400 MHz; DMSO-*d*<sub>6</sub>; TMS) δ 7.24 (d, *J* = 7.8 Hz, 1H), 7.05 (d, *J* = 7.8 Hz, 1H), 6.87 (t, *J* = 8.1 Hz, 1H), 4.29 – 4.28 (m, 4H), 3.79 (s, 3H).

**2,3-Dihydrobenzo[*b*][1,4]dioxine-5-carboxamide (4)**. Compound **4** was prepared from **14** (0.288 g, 2.0 mmol) according to general procedure A as a white powder (yield: 0.186 g, 70%); mp 130-132 °C [lit. mp 130 °C] [25]. <sup>1</sup>H NMR (400 MHz; DMSO-*d*<sub>6</sub>; TMS) δ 7.62 (s, 1H), 7.48 (s, 1H), 7.34 (dd, *J* = 7.9 Hz, 1.8 Hz, 1H), 6.98 (dd, *J* = 8.0 Hz, 1.7 Hz, 1H), 6.87 (t, *J* = 7.9 Hz, 1H), 4.37 - 4.35 (m, 2H), 4.28 - 4.26 (m, 2H). <sup>13</sup>C NMR (100 MHz; DMSO-*d*<sub>6</sub>; TMS): δ 165.87, 143.56, 141.91, 123.64, 122.27, 120.41, 119.53, 64.49, 63.55. HRMS (*m/z*): [M + H]<sup>+</sup> calcd for C<sub>9</sub>H<sub>10</sub>NO<sub>3</sub>, 180.0655; found: 180.0634.

**7-Nitro-2,3-dihydrobenzo[*b*][1,4]dioxine-5-carboxamide (15)** [15]. A solution of **4** (0.540 g, 3.0 mmol) in 5 mL (65.3 mmol) of trifluoroacetic acid was cooled in an ice bath, and 1.2 mL (28.8 mL) nitric acid was added dropwise. The reaction mixture was stirred for 6 h, and then poured into ice water. The precipitate was filtered and the crude product was purified using flash chromatography and subsequently reprecipitated using ethyl acetate and hexane to obtain pure compound **15** as a yellow powder (yield: 0.061 g, 9%);  $^1\text{H}$  NMR (400 MHz; DMSO- $d_6$ ; TMS)  $\delta$  8.13 (d,  $J = 2.8$  Hz, 1H), 7.86 (s, 1H), 7.82 (d,  $J = 2.8$  Hz, 1H), 7.62 (s, 1H), 4.49 (d,  $J = 3.9$  Hz, 2H), 4.38 (d,  $J = 4.0$  Hz, 2H).  $^{13}\text{C}$  NMR (100 MHz; DMSO- $d_6$ ; TMS):  $\delta$  164.00, 147.73, 143.85, 140.09, 124.13, 117.72, 113.92, 65.21, 63.65.

**8-Nitro-2,3-dihydrobenzo[*b*][1,4]dioxine-5-carboxamide (16)**. Compound **16** was isolated from the above-mentioned nitration reaction of **4** as yellow powder (yield: 0.088 g, 13%);  $^1\text{H}$  NMR (400 MHz; DMSO- $d_6$ ; TMS)  $\delta$  7.86 (s, 1H), 7.69 (d,  $J = 9.1$  Hz, 1H), 7.62 (s, 1H), 7.07 (d,  $J = 9.1$  Hz, 1H), 4.39 - 4.37 (m, 2H), 4.34 - 4.32 (m, 2H).

**7-Amino-2,3-dihydrobenzo[*b*][1,4]dioxine-5-carboxamide (17)** [15]. To a solution of **15** (0.448 g, 2.0 mmol) in 30 mL methanol, Pd/C (0.04 g) was added. The mixture was stirred under 4 atmosphere of hydrogen gas at room temperature for 8 h. After a halt in pressure drop, the suspension was filtered through celite pad. The filtrate was concentrated, diluted with ethyl acetate and washed with water. Ethyl acetate layer was dried over magnesium sulfate and evaporated under vacuum. The crude product was purified using flash chromatography (methanol:dichloromethane 5:95) to obtain **17** as a pale brown powder (yield: 0.233 g, 60%).  $^1\text{H}$  NMR (400 MHz; DMSO- $d_6$ ; TMS)  $\delta$  7.44 (s, 1H), 7.39 (s, 1H), 6.64 (d,  $J = 2.8$  Hz, 1H), 6.22 (d,  $J = 2.8$  Hz, 1H), 4.79 (s, 2H), 4.23 - 4.19 (m, 4H).  $^{13}\text{C}$  NMR (100 MHz; DMSO- $d_6$ ; TMS):  $\delta$

166.08, 143.75, 142.22, 132.89, 123.05, 108.23, 105.29, 64.14, 63.83. HRMS ( $m/z$ ):  $[M + H]^+$  calcd for  $C_9H_{11}N_2O_3$ , 195.0764; found: 195.0747.

**8-Amino-2,3-dihydrobenzo[*b*][1,4]dioxine-5-carboxamide (18).** Compound **18** was prepared following the procedure used for synthesis of **17**, using **16** (0.448 g, 2.0 mmol) as a starting material. Compound **18** (yield: 0.272 g, 70%) was isolated as a light brown powder.  $^1H$  NMR (400 MHz; DMSO- $d_6$ ; TMS)  $\delta$  7.47 (s, 1H), 7.36 (s, 1H), 6.66 (d,  $J = 8.9$  Hz, 1H), 6.20 (d,  $J = 8.9$  Hz, 1H), 5.78 (s, 2H), 4.26 - 4.25 (m, 2H), 4.12 - 4.10 (m, 2H). HRMS ( $m/z$ ):  $[M + H]^+$  calcd for  $C_9H_{11}N_2O_3$ , 195.0764; found: 195.0741.

**Methyl (S)-2-(Hydroxymethyl)-2,3-dihydrobenzo[*b*][1,4]dioxine-5-carboxylate (19a)** [16]. Commercially available (2*S*)-glycidyl tosylate (0.456 g, 2.0 mmol) was added to a suspension of **13** (0.336 g, 2.0 mmol) and  $K_2CO_3$  (0.304 g, 2.2 mmol) in 10 mL dimethylformamide. The mixture was stirred for 30 h at 40 °C, diluted with water and extracted with ethyl acetate. Ethyl acetate layer was dried over magnesium sulfate, and concentrated under reduced pressure. Flash chromatography (methanol:dichloromethane 5:95) was used to obtain **19a** (yield: 0.089 g, 20%) as a white solid.  $^1H$  NMR (400 MHz; DMSO- $d_6$ ; TMS)  $\delta$  7.36 (dd,  $J = 7.9$  Hz, 1.6 Hz, 1H), 7.00 (dd,  $J = 8.1$  Hz, 1.6 Hz, 1H), 6.81 (t,  $J = 7.9$  Hz, 1H), 4.42 (dd,  $J = 11.6$  Hz, 2.2 Hz, 1H), 4.28 - 4.23 (m, 1H), 4.15 - 4.05 (m, 4H), 3.84 (s, 3H).

**Methyl (R)-3-(hydroxymethyl)-2,3-dihydrobenzo[*b*][1,4]dioxine-5-carboxylate (19b).** From the same reaction of intermediate **13** (0.336 g, 2.0 mmol) and (2*S*)-glycidyl tosylate (0.456 g, 2.0 mmol), compound **19b** (yield: 0.116 g, 26%) was isolated as a white solid.  $^1H$  NMR (400 MHz; DMSO- $d_6$ ; TMS)  $\delta$  7.73 (dd,  $J = 7.9$  Hz, 1.7 Hz, 1H), 7.17 (dd,  $J = 8.0$  Hz, 1.7 Hz, 1H), 7.02 (t,  $J$

= 8.0 Hz, 1H), 4.61 (dd,  $J = 15.2$  Hz, 6.6 Hz, 1H), 4.41 - 4.34 (m, 2H), 4.03 - 3.91 (m, 3H), 3.83 (s, 3H).

**(S)-2-(Hydroxymethyl)-2,3-dihydrobenzo[*b*][1,4]dioxine-5-carboxamide (20a).** Compound **20a** was prepared according to general procedure A, starting with **19a** (0.448 g, 2.0 mmol). Purified compound **20a** (yield: 0.293 g, 70%) was obtained as a white powder, mp 142-144 °C.  $^1\text{H}$  NMR (400 MHz; DMSO- $d_6$ ; TMS)  $\delta$  7.54 (s, 2H), 7.27 (dd,  $J = 7.8$  Hz, 1.7 Hz, 1H), 6.99 (dd,  $J = 8.0$  Hz, 1.7 Hz, 1H), 6.87 (t,  $J = 7.8$  Hz, 1H), 5.10 (t,  $J = 5.7$  Hz, 1H), 4.45 (dd,  $J = 9.3$  Hz, 2.1 Hz, 1H), 4.21 - 4.16 (m, 1H), 4.11 - 4.06 (m, 1H), 3.69 - 3.58 (m, 2H). HRMS ( $m/z$ ):  $[\text{M} + \text{H}]^+$  calcd for  $\text{C}_{10}\text{H}_{12}\text{NO}_4$ , 210.0761; found: 210.0753. ee = 94%, ( $t_{\text{R}}$  (major) = 10.42,  $t_{\text{R}}$  (minor) = 9.77).

**(R)-3-(Hydroxymethyl)-2,3-dihydrobenzo[*b*][1,4]dioxine-5-carboxamide (20b).** Compound **20b** was prepared according to general procedure A, starting with **19b** (0.448 g, 2.0 mmol). Purified compound **20b** (yield: 0.251 g, 60%) was obtained as a white powder, mp 144-146 °C.  $^1\text{H}$  NMR (400 MHz; DMSO- $d_6$ ; TMS)  $\delta$  7.61 (s, 1H), 7.55 (s, 1H), 7.37 (dd,  $J = 7.8$  Hz, 1.7 Hz, 1H), 7.01 (dd,  $J = 8.0$  Hz, 1.7 Hz, 1H), 6.88 (t,  $J = 7.9$  Hz, 1H), 5.19 (t,  $J = 11.5$  Hz, 1H), 4.36 (dd,  $J = 8.7$  Hz, 2.6 Hz, 1H), 4.32 - 4.27 (m, 1H), 4.08 - 4.03 (m, 1H), 3.74 - 3.63 (m, 2H). HRMS ( $m/z$ ):  $[\text{M} + \text{H}]^+$  calcd for  $\text{C}_{10}\text{H}_{12}\text{NO}_4$ , 210.0761; found: 210.0744. ee = 93%, ( $t_{\text{R}}$  (major) = 7.43,  $t_{\text{R}}$  (minor) = 9.01).

**(R)-(5-Carbamoyl-2,3-dihydrobenzo[*b*][1,4]dioxin-2-yl)methyl methanesulfonate (21a)** [26]. Methanesulfonyl chloride (0.15 mL, 2.0 mmol) was added to a solution of **20a** (0.518 g, 2.0 mmol) and triethylamine (0.3 mL, 2.2 mmol) in 20 mL dichloromethane at -10 °C. The mixture was stirred for 10 h at room temperature, and the reaction mixture was washed with water. Then

the combined organic portion was dried over magnesium sulfate, and concentrated under vacuum. After purification with column chromatography, compound **21a** (yield: 0.356 g, 50%) was obtained as a white solid, mp 145-147 °C. <sup>1</sup>H NMR (400 MHz; DMSO-*d*<sub>6</sub>; TMS) δ 7.56 (br, 2H), 7.29 (dd, *J* = 7.7 Hz, 1.5 Hz, 1H), 7.05 (dd, *J* = 7.9 Hz, 1.5 Hz, 1H), 6.92 (t, *J* = 7.9 Hz, 1H), 4.56 - 4.43 (m, 4H), 4.18 - 4.13 (m, 1H), 3.26 (s, 3H). HRMS (*m/z*): [M + H]<sup>+</sup> calcd for C<sub>11</sub>H<sub>14</sub>NO<sub>6</sub>S, 288.0536; found: 288.0540. ee = 94%, (*t*<sub>R</sub> (major) 11.71, *t*<sub>R</sub> (minor) = 13.05).

**(S)-(8-Carbamoyl-2,3-dihydrobenzo[*b*][1,4]dioxin-2-yl)methyl methanesulfonate (21b).**

Compound **21b** was prepared following the procedure used for the synthesis of **21a**, using **20b** (0.287 g, 1.0 mmol) as a starting material. Purified compound **21b** (yield: 0.217 g, 55%) was obtained as a white solid, mp 140-143 °C. <sup>1</sup>H NMR (400 MHz; DMSO-*d*<sub>6</sub>; TMS) δ 7.64 (s, 1H), 7.47 (s, 1H), 7.35 (d, *J* = 7.8 Hz, 1H), 7.04 (d, *J* = 7.8 Hz, 1H), 6.92 (t, *J* = 7.8 Hz, 1H), 4.63 (d, *J* = 10.1 Hz 2H), 4.51 (dd, *J* = 11.6 Hz, 5.7 Hz, 1H), 4.44 (d, *J* = 11.1 Hz, 1H), 4.09 (dd, *J* = 11.2 Hz, 7.7 Hz 1H), 3.26 (s, 3H). HRMS (*m/z*): [M + H]<sup>+</sup> calcd for C<sub>11</sub>H<sub>14</sub>NO<sub>6</sub>S, 288.0536; found: 288.0511. ee = 93%, (*t*<sub>R</sub> (major) 12.88, *t*<sub>R</sub> (minor) = 13.59).

**(S)-2-((4-Methylpiperazin-1-yl)methyl)-2,3-dihydrobenzo[*b*][1,4]dioxine-5-carboxamide**

**(22a)** [27]. A mixture of **21a** (0.287 g, 1.0 mmol) and *N*-methylpiperazine (0.33 mL, 3.0 mmol) in ethanol was stirred for 10 h under reflux. Ethanol was then removed under vacuum. The concentrated mass was diluted with water, and extracted with ethyl acetate at potassium carbonate-assisted alkaline pH. After drying over magnesium sulfate, the organic layer was concentrated under reduced pressure and purified using preparative TLC (methanol:dichloromethane = 5: 95) to obtain compound **22a** (yield: 0.058 g, 20%) as a white solid, mp 173-175 °C. <sup>1</sup>H NMR (400 MHz, Chloroform-*d*) δ 7.74 (dd, *J* = 7.8 Hz, 1.8 Hz, 1H), 7.52 (s, 1H), 7.04 (dd, *J* = 8.1 Hz, 1.8 Hz, 1H), 6.94 (t, *J* = 7.8 Hz, 1H), 5.76 (br, 1H), 4.50 (dd, *J*

= 11.1 Hz, 2.3 Hz, 1H), 4.38 - 4.32 (m, 1H), 4.13 (dd,  $J = 11.3$  Hz, 10.0 Hz, 1H), 2.76 - 2.45 (m, 10H), 2.30 (s, 3H). HRMS ( $m/z$ ):  $[M + H]^+$  calcd for  $C_{15}H_{22}N_3O_3$ , 292.1656; found: 292.1685.

**(R)-3-((4-Methylpiperazin-1-yl)methyl)-2,3-dihydrobenzo[*b*][1,4]dioxine-5-carboxamide**

**(22b)**. Compound **22b** was synthesized according to the procedure for compound **22a**, starting with **21b** (0.287 g, 1.0 mmol) and *N*-methylpiperazine (0.33 mL, 3.0 mmol). The mixture was purified using preparative TLC to obtain compound **22b** (yield: 0.070 g, 24%) as a white solid, mp 185-187 °C.  $^1H$  NMR (400 MHz, Chloroform-*d*)  $\delta$  7.76 (dd,  $J = 8.1$  Hz, 1.9 Hz, 1H), 7.46 (s, 1H), 7.08 (dd,  $J = 8.1$  Hz, 1.7 Hz, 1H), 6.97 (t,  $J = 8.0$  Hz, 1H), 5.75 (br, 1H), 4.51 - 4.35 (m, 4H), 4.20 (dd,  $J = 8.5$  Hz, 6.7 Hz, 1H), 3.50 (s, 4H), 2.39 - 2.30 (m, 7H). HRMS ( $m/z$ ):  $[M + H]^+$  calcd for  $C_{15}H_{22}N_3O_3$ , 292.1656; found: 292.1629.

**(S)-2-((4-(Pyrimidin-2-yl)piperazin-1-yl)methyl)-2,3-dihydrobenzo[*b*][1,4]dioxine-5-**

**carboxamide (23a)**. Compound **23a** was synthesized according to the procedure used to obtain compound **22a**, starting with **21a** (0.287 g, 1.0 mmol) and 1-(2-pyrimidinyl)piperazine (0.43 mL, 3.0 mmol). Compound **23a** (yield: 0.117 g, 33%) was isolated as a white solid, mp 180-182 °C.  $^1H$  NMR (400 MHz, Chloroform-*d*)  $\delta$  8.31 (d,  $J = 4.8$  Hz, 2H), 7.76 (dd,  $J = 7.8$  Hz, 1.9 Hz, 1H), 7.52 (s, 1H), 7.05 (dd,  $J = 8.1$  Hz, 1.8 Hz, 1H), 6.96 (t,  $J = 7.9$  Hz, 1H), 6.50 (t,  $J = 4.8$  Hz, 1H), 5.73 (br, 1H), 4.56 (dd,  $J = 11.6$  Hz, 2.5 Hz, 1H), 4.40 (t,  $J = 6.1$  Hz, 1H), 4.56 (dd,  $J = 11.3$  Hz, 9.5 Hz, 1H), 3.84 (t,  $J = 4.9$  Hz, 4H), 2.80 - 2.57 (m, 6H). HRMS ( $m/z$ ):  $[M + H]^+$  calcd for  $C_{18}H_{22}N_5O_3$ , 356.1717; found: 356.1736.

**(R)-3-((4-(Pyrimidin-2-yl)piperazin-1-yl)methyl)-2,3-dihydrobenzo[*b*][1,4]dioxine-5-**

**carboxamide (23b)**. Compound **23b** was synthesized according to the procedure reported for compound **22a**, starting with **21b** (0.287 g, 1.0 mmol) and 1-(2-pyrimidinyl)piperazine (0.43 mL,

3.0 mmol). Compound **23b** (yield: 0.135 g, 38%) was isolated as a white solid, mp 155-157 °C. <sup>1</sup>H NMR (400 MHz, Chloroform-*d*) δ 8.33 (d, *J* = 4.7 Hz, 2H), 7.76 (dd, *J* = 7.8 Hz, 1.8 Hz, 1H), 7.46 (s, 1H), 7.09 (dd, *J* = 8.0 Hz, 1.7 Hz, 1H), 6.98 (t, *J* = 8.0 Hz, 1H), 6.54 (t, *J* = 4.8 Hz, 1H), 5.75 (br, 1H), 4.54 - 4.42 (m, 4H), 4.23 (dd, *J* = 12.0 Hz, 10.8 Hz, 1H), 3.83 (s, 4H), 3.54 (dd, *J* = 12.7 Hz, 6.3 Hz, 4H). HRMS (*m/z*): [M + H]<sup>+</sup> calcd for C<sub>18</sub>H<sub>22</sub>N<sub>5</sub>O<sub>3</sub>, 356.1717; found: 356.1711.

**Methyl (R)-2-(hydroxymethyl)-2,3-dihydrobenzo[*b*][1,4]dioxine-5-carboxylate (24a).**

Compound **24a** was prepared by the procedure used for the synthesis of **19a**, with **13** (0.336 g, 2.0 mmol) and (2*R*)-glycidyl tosylate (0.456 g, 2.0 mmol) as starting materials. Intermediate **24a** (yield: 0.098 g, 22%) was isolated as a white powder. <sup>1</sup>H NMR (400 MHz; DMSO-*d*<sub>6</sub>; TMS) δ 7.35 (dd, *J* = 7.9 Hz, 1.6 Hz, 1H), 7.00 (dd, *J* = 8.1 Hz, 1.6 Hz, 1H), 6.81 (t, *J* = 7.9 Hz, 1H), 4.42 (dd, *J* = 11.6 Hz, 2.1 Hz, 1H), 4.28 - 4.20 (m, 1H), 4.15 - 4.05 (m, 4H), 3.83 (s, 3H).

**Methyl (S)-3-(hydroxymethyl)-2,3-dihydrobenzo[*b*][1,4]dioxine-5-carboxylate (24b).**

Compound **24b** was isolated from the same reaction from which **24a** was obtained. Crude product was purified to yield compound **24b** (yield: 0.157 g, 35%) as a white solid. <sup>1</sup>H NMR (400 MHz; DMSO-*d*<sub>6</sub>; TMS) δ 7.73 (dd, *J* = 7.9 Hz, 1.7 Hz, 1H), 7.17 (dd, *J* = 7.9 Hz, 1.7 Hz, 1H), 7.02 (t, *J* = 8.0 Hz, 1H), 4.61 (dd, *J* = 15.2 Hz, 6.6 Hz, 1H), 4.43 - 4.34 (m, 2H), 4.05 - 3.91 (m, 3H), 3.83 (s, 3H).

**(R)-2-(Hydroxymethyl)-2,3-dihydrobenzo[*b*][1,4]dioxine-5-carboxamide (25a).**

Compound **25a** was prepared according to general procedure A, starting with **24a** (0.448 g, 2.0 mmol). Crude product was purified to yield compound **25a** (yield: 0.251 g, 60%) as a white powder, mp 142-144 °C. <sup>1</sup>H NMR (400 MHz; DMSO-*d*<sub>6</sub>; TMS) δ 7.54 (s, 2H), 7.27 (dd, *J* = 8.1 Hz, 1.7 Hz,

1H), 6.99 (dd,  $J = 8.0$  Hz, 1.7 Hz, 1H), 6.87 (t,  $J = 7.9$  Hz, 1H), 5.10 (t,  $J = 5.7$  Hz, 1H), 4.45 (dd,  $J = 9.3$  Hz, 2.1 Hz, 1H), 4.21 - 4.16 (m, 1H), 4.11 - 4.06 (m, 1H), 3.69 - 3.58 (m, 2H). HRMS ( $m/z$ ):  $[M + H]^+$  calcd for  $C_{10}H_{12}NO_4$ , 210.0761; found: 210.0772. ee = 93%, ( $t_R$  (major) = 9.75,  $t_R$  (minor) = 10.42).

**(S)-3-(Hydroxymethyl)-2,3-dihydrobenzo[*b*][1,4]dioxine-5-carboxamide (25b).** Compound **25b** was prepared according to general procedure A, starting with **24b** (0.448 g, 2.0 mmol). Crude product was purified to yield compound **25b** (yield: 0.293 g, 70%) as a white solid, mp 144-146 °C.  $^1H$  NMR (400 MHz; DMSO- $d_6$ ; TMS)  $\delta$  7.61 (s, 1H), 7.55 (s, 1H), 7.37 (dd,  $J = 8.0$  Hz, 1.7 Hz, 1H), 7.01 (dd,  $J = 7.9$  Hz, 1.7 Hz, 1H), 6.88 (t,  $J = 7.9$  Hz, 1H), 5.19 (t,  $J = 5.8$  Hz, 1H), 4.36 (dd,  $J = 8.7$  Hz, 2.6 Hz, 1H), 4.32 - 4.27 (m, 1H), 4.08 - 4.03 (m, 1H), 3.74 - 3.63 (m, 2H). HRMS ( $m/z$ ):  $[M + H]^+$  calcd for  $C_{10}H_{12}NO_4$ , 210.0761; found: 210.0752. ee = 92%, ( $t_R$  (major) 8.92,  $t_R$  (minor) = 7.40).

**(S)-(5-Carbamoyl-2,3-dihydrobenzo[*b*][1,4]dioxin-2-yl)methyl methanesulfonate (26a).** Compound **26a** was prepared by the procedure used for the synthesis of **21a** using **25a** (0.287 g, 1.0 mmol) as the starting material. Crude product was purified to yield compound **26a** (yield: 0.197 g, 50%) as a white solid, mp 145-147 °C.  $^1H$  NMR (400 MHz; DMSO- $d_6$ ; TMS)  $\delta$  7.56 (br, 2H), 7.29 (dd,  $J = 7.9$  Hz, 1.5 Hz, 1H), 7.05 (dd,  $J = 7.9$  Hz, 1.5 Hz, 1H), 6.92 (t,  $J = 7.8$  Hz, 1H), 4.56-4.43 (m, 4H), 4.16 (dd,  $J = 11.5$  Hz, 6.8 Hz, 1H), 3.26 (s, 3H). ee = 93%, ( $t_R$  (major) 13.05,  $t_R$  (minor) = 11.72).

**(R)-(8-Carbamoyl-2,3-dihydrobenzo[*b*][1,4]dioxin-2-yl)methyl methanesulfonate (26b).** Compound **26b** was prepared by the procedure used for the synthesis of **21a** using **25b** (0.287 g, 1.0 mmol) as the starting material. Crude product was purified to yield compound **26b** (yield:

0.217 g, 55%) as a white solid, mp 140-143 °C. <sup>1</sup>H NMR (400 MHz; DMSO-*d*<sub>6</sub>; TMS) δ 7.64 (s, 1H), 7.47 (s, 1H), 7.36 (d, *J* = 7.9 Hz, 1H), 7.04 (d, *J* = 8.1 Hz, 1H), 6.92 (t, *J* = 7.7 Hz, 1H), 4.63 (d, *J* = 10.8 Hz, 2H), 4.53 - 4.49 (m, 1H), 4.44 (d, *J* = 11.9 Hz, 1H), 4.09 (dd, *J* = 10.7 Hz, 7.5 Hz, 1H), 3.26 (s, 3H). HRMS (*m/z*): [M + H]<sup>+</sup> calcd for C<sub>11</sub>H<sub>14</sub>NO<sub>6</sub>S, 288.0536; found: 288.0517. ee = 92%, (*t*<sub>R</sub> (major) 13.59, *t*<sub>R</sub> (minor) = 12.88).

**(*R*)-2-((4-Methylpiperazin-1-yl)methyl)-2,3-dihydrobenzo[*b*][1,4]dioxine-5-carboxamide**

**(27a).** Compound **27a** was synthesized according to the procedure used for compound **22a** using **26a** (0.287 g, 1.0 mmol) and *N*-methylpiperazine (0.33 mL, 3.0 mmol) as the starting materials. Crude product was purified to yield compound **27a** (yield: 0.058 g, 20%) as white solid, mp 173-175 °C. <sup>1</sup>H NMR (400 MHz, Chloroform-*d*) δ 7.74 (dd, *J* = 7.8 Hz, 1.8 Hz, 1H), 7.52 (s, 1H), 7.04 (dd, *J* = 8.1 Hz, 1.8 Hz, 1H), 6.94 (t, *J* = 7.8 Hz, 1H), 5.76 (br, 1H), 4.50 (dd, *J* = 11.1 Hz, 2.3 Hz, 1H), 4.38 - 4.32 (m, 1H), 4.13 (dd, *J* = 11.3 Hz, 10.0 Hz, 1H), 2.76 - 2.45 (m, 10H), 2.30 (s, 3H). HRMS (*m/z*): [M + H]<sup>+</sup> calcd for C<sub>15</sub>H<sub>22</sub>N<sub>3</sub>O<sub>3</sub>, 292.1656; found: 292.1637.

**(*S*)-3-((4-Methylpiperazin-1-yl)methyl)-2,3-dihydrobenzo[*b*][1,4]dioxine-5-carboxamide**

**(27b).** Compound **27b** was synthesized according to the procedure reported for compound **22a** using **26b** (0.287 g, 1.0 mmol) and *N*-methylpiperazine (0.33 mL, 3.0 mmol) as the starting materials. Crude product was purified to yield compound **27b** (yield: 0.058 g, 20%) as a white solid, mp 185-187 °C. <sup>1</sup>H NMR (400 MHz, Chloroform-*d*) δ 7.76 (dd, *J* = 8.1 Hz, 1.9 Hz, 1H), 7.46 (s, 1H), 7.08 (dd, *J* = 8.1 Hz, 1.7 Hz, 1H), 6.97 (t, *J* = 8.0 Hz, 1H), 5.75 (br, 1H), 4.51 - 4.35 (m, 4H), 4.20 (dd, *J* = 8.5 Hz, 6.7 Hz, 1H), 3.50 (s, 4H), 2.39 - 2.30 (m, 7H). HRMS (*m/z*): [M + H]<sup>+</sup> calcd for C<sub>15</sub>H<sub>22</sub>N<sub>3</sub>O<sub>3</sub>, 292.1656; found: 292.1685.

**(R)-2-((4-(Pyrimidin-2-yl)piperazin-1-yl)methyl)-2,3-dihydrobenzo[*b*][1,4]dioxine-5-carboxamide (28a).** Compound **28a** was synthesized according to the procedure used for **22a** with **26a** (0.287 g, 1.0 mmol) and 1-(2-pyrimidinyl)piperazine (0.43 mL, 3.0 mmol) as the starting materials. Crude product was purified to yield compound **28a** (yield: 0.092 g, 26%) as a white solid, mp 180-182 °C. <sup>1</sup>H NMR (400 MHz, Chloroform-*d*) δ 8.31 (d, *J* = 4.8 Hz, 2H), 7.76 (dd, *J* = 7.8 Hz, 1.9 Hz, 1H), 7.52 (s, 1H), 7.05 (dd, *J* = 8.1 Hz, 1.8 Hz, 1H), 6.96 (t, *J* = 7.9 Hz, 1H), 6.50 (t, *J* = 4.8 Hz, 1H), 5.73 (br, 1H), 4.56 (dd, *J* = 11.6 Hz, 2.5 Hz, 1H), 4.40 (t, *J* = 6.1 Hz, 1H), 4.56 (dd, *J* = 11.3 Hz, 9.5 Hz, 1H), 3.84 (t, *J* = 4.9 Hz, 4H), 2.80 - 2.57 (m, 6H). HRMS (*m/z*): [M + H]<sup>+</sup> calcd for C<sub>18</sub>H<sub>22</sub>N<sub>5</sub>O<sub>3</sub>, 356.1717; found: 356.1702.

**(S)-3-((4-(Pyrimidin-2-yl)piperazin-1-yl)methyl)-2,3-dihydrobenzo[*b*][1,4]dioxine-5-carboxamide (28b).** Compound **28b** was synthesized according to the procedure for compound **22a** with **26b** (0.287 g, 1.0 mmol) and 1-(2-pyrimidinyl)piperazine (0.43 mL, 3.0 mmol) as the starting materials. Crude product was purified to yield compound **28b** (yield: 0.110 g, 31%) as a white solid, mp 155-157 °C. <sup>1</sup>H NMR (400 MHz, Chloroform-*d*) δ 8.33 (d, *J* = 4.7 Hz, 2H), 7.76 (dd, *J* = 7.8 Hz, 1.8 Hz, 1H), 7.46 (s, 1H), 7.09 (dd, *J* = 8.0 Hz, 1.7 Hz, 1H), 6.98 (t, *J* = 8.0 Hz, 1H), 6.54 (t, *J* = 4.8 Hz, 1H), 5.75 (br, 1H), 4.54 - 4.42 (m, 4H), 4.23 (dd, *J* = 12.0 Hz, 10.8 Hz, 1H), 3.83 (s, 4H), 3.54 (dd, *J* = 12.7 Hz, 6.3 Hz, 4H). HRMS (*m/z*): [M + H]<sup>+</sup> calcd for C<sub>18</sub>H<sub>22</sub>N<sub>5</sub>O<sub>3</sub>, 356.1717; found: 356.1698.

**Methyl benzo[*d*][1,3]dioxole-4-carboxylate (29).** Compound **29** was prepared in the same manner as **14**, using **13** (0.336 g, 2.0 mmol) and dibromomethane (0.14 mL, 2.0 mmol) as starting materials. Crude product was purified to yield compound **29** (yield: 0.234 g, 65%) as a

white powder.  $^1\text{H}$  NMR (400 MHz; DMSO- $d_6$ ; TMS)  $\delta$  7.30 (dd,  $J = 8.1$  Hz, 1.2 Hz, 1H), 7.16 (dd,  $J = 7.7$  Hz, 1.2 Hz, 1H), 6.93 (t,  $J = 7.8$  Hz, 1H), 6.15 (s, 2H), 3.82 (s, 3H).

**Methyl 3,4-dihydro-2H-benzo[*b*][1,4]dioxepine-6-carboxylate (30).** Compound **30** was prepared by the procedure for **14**, using **13** (0.336 g, 2.0 mmol) and 1,3-dibromopropane (0.21 mL, 2.0 mmol) as starting materials. Crude product was purified to yield compound **30** (yield: 0.229 g, 55%) as a white powder.  $^1\text{H}$  NMR (400 MHz; DMSO- $d_6$ ; TMS)  $\delta$  7.34 (dd,  $J = 7.8$  Hz, 1.8 Hz, 1H), 7.08 (dd,  $J = 8.0$  Hz, 1.8 Hz, 1H), 6.99 (t,  $J = 7.8$  Hz, 1H), 4.28 (t,  $J = 5.3$  Hz, 2H), 4.13 (t,  $J = 5.3$  Hz, 2H), 2.15 - 2.09 (m, 2H), 3.77 (s, 3H).

**Benzo[*d*][1,3]dioxole-4-carboxamide (31).** Compound **31** was prepared according to general procedure A, starting with **29** (0.360 g, 2.0 mmol). Crude product was purified to yield compound **31** (yield: 0.198 g, 60%) as a white solid.  $^1\text{H}$  NMR (400 MHz; DMSO- $d_6$ ; TMS)  $\delta$  7.65 (s, 1H), 7.25 (d,  $J = 8.0$  Hz, 1H), 7.16 (s, 1H), 7.07 (d,  $J = 7.7$  Hz, 1H), 6.91 (t,  $J = 7.9$  Hz, 1H), 6.13 (s, 2H). HRMS ( $m/z$ ):  $[\text{M} + \text{H}]^+$  calcd for  $\text{C}_8\text{H}_8\text{NO}_3$ , 166.0499; found: 166.0477.

**3,4-Dihydro-2H-benzo[*b*][1,4]dioxepine-6-carboxamide (32).** Compound **32** was prepared according to general procedure A, using **30** (0.416 g, 2.0 mmol) as the starting material. Crude product was purified to yield compound **32** (yield: 0.232 g, 60%) as a white powder, mp 106-108 °C.  $^1\text{H}$  NMR (400 MHz; DMSO- $d_6$ ; TMS)  $\delta$  7.62 (s, 1H), 7.48 (s, 1H), 7.34 (dd,  $J = 7.9$  Hz, 1.8 Hz, 1H), 7.08 (dd,  $J = 8.0$  Hz, 1.8 Hz, 1H), 6.99 (t,  $J = 7.8$  Hz, 1H), 4.23 (t,  $J = 5.5$  Hz, 2H), 4.14 (t,  $J = 5.4$  Hz, 2H), 2.16 - 2.10 (m, 2H).  $^{13}\text{C}$  NMR (100 MHz; DMSO- $d_6$ ; TMS):  $\delta$  166.69, 151.75, 149.38, 128.67, 123.90, 123.70, 122.89, 70.89, 70.42, 31.15. HRMS ( $m/z$ ):  $[\text{M} + \text{H}]^+$  calcd for  $\text{C}_{10}\text{H}_{12}\text{NO}_3$ , 194.0812; found: 194.0799.

**Methyl 2-hydroxy-3-nitrobenzoate (34).** Compound **34** was prepared by the procedure for **13** using commercially available 2-hydroxy-3-nitrobenzoic acid **33** (0.366 g, 2.0 mmol) as the starting material. Crude product was purified to yield compound **34** (yield: 0.347 g, 88%) as a white powder.  $^1\text{H}$  NMR (400 MHz; DMSO- $d_6$ ; TMS)  $\delta$  11.48 (s, 1H), 8.18 (dd,  $J$  = 8.1 Hz, 1.7 Hz, 1H), 8.09 (dd,  $J$  = 7.9 Hz, 1.7 Hz, 1H), 7.11 (t,  $J$  = 8.1 Hz, 1H), 3.93 (s, 3H).

**Methyl 2-(2-ethoxy-2-oxoethoxy)-3-nitrobenzoate (35)** [18]. Ethyl bromoacetate (0.12 mL, 1.1 mmol) and  $\text{K}_2\text{CO}_3$  (0.276 g, 2.0 mmol) were added to a solution of compound **34** (0.197 g, 1.0 mmol) in 10 mL dimethylformamide. After stirring for 8 h at room temperature, the mixture was diluted with ethyl acetate, and washed with water. Pure product **35** (yield: 0.212 g, 75%) was obtained by flash chromatography (methanol:dichloromethane 10:90) as a white solid.  $^1\text{H}$  NMR (400 MHz; chloroform- $d$ )  $\delta$  8.10 (dd,  $J$  = 6.3 Hz, 1.6 Hz, 1H), 7.99 (dd,  $J$  = 8.0 Hz, 1.3 Hz, 1H), 7.36 (t,  $J$  = 8.1 Hz, 1H), 4.82 (s, 2H), 4.30 (q,  $J$  = 7.2 Hz, 2H), 3.94 (s, 3H), 1.32 (t,  $J$  = 7.1 Hz, 3H).

**Methyl 2-(2-ethoxy-2-oxo-1-phenylethoxy)-3-nitrobenzoate (36).** Compound **36** was prepared in a similar manner as **35** using compound **34** (0.197 g, 1.0 mmol) and commercially available ethyl 2-bromo-2-phenylacetate (0.267 g, 1.1 mmol) as the starting materials. Purification by column chromatography using ethyl acetate:hexane mixture as an eluent yielded compound **36** (yield: 0.280 g, 78%) as a yellow oil.  $^1\text{H}$  NMR (400 MHz, Chloroform- $d$ )  $\delta$  7.98 (dd,  $J$  = 7.9 Hz, 1.7 Hz, 1H), 7.84 (dd,  $J$  = 8.0 Hz, 1.9 Hz, 1H), 7.46 - 7.37 (m, 2H), 7.37 - 7.28 (m, 3H), 7.22 (t,  $J$  = 8.0 Hz, 1H), 5.58 (s, 1H), 4.10 (q,  $J$  = 7.1 Hz, 2H), 3.79 (s, 3H), 1.10 (t,  $J$  = 7.1 Hz, 3H).

**Methyl 2-(2-ethoxy-1-(4-methoxyphenyl)-2-oxoethoxy)-3-nitrobenzoate (37).** Compound **37** was prepared as for **35** using compound **34** (0.197 g, 1.0 mmol) and commercially available ethyl

2-bromo-2-(4-methoxyphenyl)acetate (0.301 g, 1.1 mmol) as the starting materials. Purification of crude product by column chromatography using ethyl acetate:hexane mixture as an eluent yielded compound **37** (yield: 0.269 g, 69%) as a dark yellow colored oil.  $^1\text{H NMR}$  (400 MHz,  $\text{DMSO-}d_6$ )  $\delta$  8.05 (td,  $J = 8.0$  Hz, 1.8 Hz, 2H), 7.42 (t,  $J = 8.0$  Hz, 1H), 7.33 - 7.27 (m, 2H), 6.98 - 6.90 (m, 2H), 5.63 (s, 1H), 4.09 (q,  $J = 7.1$  Hz, 2H), 3.81 (s, 3H), 3.76 (s, 3H), 1.08 (t,  $J = 7.1$  Hz, 3H).

**Methyl 2-(1-(4-bromophenyl)-2-ethoxy-2-oxoethoxy)-3-nitrobenzoate (38).** Compound **38** was prepared as for **35** using compound **34** (0.197 g, 1.0 mmol) and commercially available ethyl 2-bromo-2-(4-bromophenyl)acetate (0.354 g, 1.1 mmol) as the starting materials. Purification of crude product by column chromatography using ethyl acetate:hexane mixture as an eluent yielded compound **38** (yield: 0.368 g, 84%) as a brown colored oil.  $^1\text{H NMR}$  (400 MHz,  $\text{DMSO-}d_6$ )  $\delta$  8.16 – 8.03 (m, 2H), 7.63 (d,  $J = 8.2$  Hz, 2H), 7.46 (t,  $J = 7.9$  Hz, 1H), 7.36 (d,  $J = 8.3$  Hz, 2H), 5.74 (br, 1H), 4.15 - 4.01 (m, 2H), 3.77 (s, 3H), 1.07 (t,  $J = 7.1$  Hz, 3H).

**Methyl 3-oxo-3,4-dihydro-2H-benzo[*b*][1,4]oxazine-8-carboxylate (39).** Iron (0.283 g) was added into a solution of **35** (0.283 g, 1.0 mmol) in 10 mL of acetic acid. After stirring for 4 h under reflux conditions, the reaction mixture was concentrated under vacuum and the crude product was directly loaded onto a silica gel column and purified using ethyl acetate:hexane mixture to obtain **39** (yield: 0.145 g, 70%) as a white solid.  $^1\text{H NMR}$  (400 MHz;  $\text{DMSO-}d_6$ )  $\delta$  10.88 (s, 1H), 7.33 (dd,  $J = 7.8$  Hz, 1.8 Hz, 1H), 7.09 (dd,  $J = 7.8$  Hz, 1.7 Hz, 1H), 7.03 (t,  $J = 7.8$  Hz, 1H), 4.65 (s, 2H), 3.80 (s, 3H).

**Methyl 3-oxo-2-phenyl-3,4-dihydro-2H-benzo[*b*][1,4]oxazine-8-carboxylate (40).** Compound **40** was prepared as for **39** using intermediate **36** (0.359 g, 1.0 mmol). The resulting mixture was purified by column chromatography using ethyl acetate:hexane mixtures as an eluent to obtain

compound **40** (yield: 0.221 g, 78%) as a white solid.  $^1\text{H}$  NMR (400 MHz,  $\text{DMSO-}d_6$ )  $\delta$  11.14 (s, 1H), 7.63 – 7.22 (m, 6H), 7.07 (dd,  $J = 23.9$  Hz, 7.8 Hz, 2H), 5.91 (s, 1H), 3.80 (s, 3H).

**Methyl 2-(4-methoxyphenyl)-3-oxo-3,4-dihydro-2H-benzo[*b*][1,4]oxazine-8-carboxylate (41).** Compound **41** was prepared as for **39** using intermediate **37** (0.389 g, 1.0 mmol). The resulting mixture was purified by column chromatography using ethyl acetate:hexane mixtures as an eluent to yield compound **41** (yield: 0.216 g, 69%) as a white solid.  $^1\text{H}$  NMR (400 MHz,  $\text{DMSO-}d_6$ )  $\delta$  11.11 (s, 1H), 7.33 (d,  $J = 7.9$  Hz, 3H), 7.16 – 6.98 (m, 2H), 6.92 (d,  $J = 8.4$  Hz, 2H), 5.82 (s, 1H), 3.79 (s, 3H), 3.73 (s, 3H).

**Methyl 2-(4-bromophenyl)-3-oxo-3,4-dihydro-2H-benzo[*b*][1,4]oxazine-8-carboxylate (42).** Compound **42** was prepared as for **39** using intermediate **38** (0.438 g, 1.0 mmol). The resulting mixture was purified by column chromatography using ethyl acetate:hexane mixtures as an eluent to obtain compound **42** (yield: 0.257 g, 78%) as a white solid.  $^1\text{H}$  NMR (400 MHz,  $\text{DMSO-}d_6$ )  $\delta$  11.18 (s, 1H), 7.80 – 7.24 (m, 5H), 7.24 – 6.91 (m, 2H), 5.92 (s, 1H), 3.81 (s, 3H).

**Methyl 3,4-dihydro-2H-benzo[*b*][1,4]oxazine-8-carboxylate (43)** [19]. A solution of **39** (0.414 g, 2.0 mmol) in 10 mL of tetrahydrofuran was treated with boron trifluoride diethyl etherate complex (0.52 mL, 4.2 mmol) in an ice bath, and  $\text{NaBH}_4$  (0.159 g, 4.2 mmol) was added after stirring for 30 min. 2M hydrochloric acid solution was used to quench the reaction, followed by extraction with ethyl acetate. The organic portion was dried over magnesium sulfate and concentrated under reduced pressure. The resulted crude product was purified using flash chromatography (ethyl acetate:hexane 30:70) to obtain **43** (yield: 0.088 g, 23%) as a white solid.  $^1\text{H}$  NMR (400 MHz;  $\text{DMSO-}d_6$ )  $\delta$  6.70-6.63 (m, 2H), 6.48 (1H, dd,  $J = 5.2$  Hz, 2.1 Hz, 1H), 4.56 (s, 1H), 4.14 (t,  $J = 4.4$  Hz, 2H), 3.97 (s, 3H), 3.23 (t,  $J = 4.4$  Hz, 2H).

**3,4-Dihydro-2H-benzo[*b*][1,4]oxazine-8-carboxamide (44).** Compound **44** was prepared according to general procedure A, starting from **43** (0.354 g, 2.0 mmol) as a white powder (yield: 0.214 g, 60%), mp 165-168 °C. <sup>1</sup>H NMR (400 MHz; DMSO-*d*<sub>6</sub>) δ 7.53 (s, 1H), 7.40 (s, 1H), 6.98 (dd, *J* = 7.9 Hz, 1.9 Hz, 1H), 6.70 (t, *J* = 7.7 Hz, 1H), 6.66 (dd, *J* = 7.8 Hz, 1.9 Hz, 1H), 5.95 (s, 1H), 4.23 (t, *J* = 4.4 Hz, 2H), 3.32-3.29 (m, 2H). HRMS (*m/z*): [M + H]<sup>+</sup> calcd for C<sub>9</sub>H<sub>11</sub>N<sub>2</sub>O<sub>2</sub>, 179.0815; found: 179.0844.

**3-Oxo-3,4-dihydro-2H-benzo[*b*][1,4]oxazine-8-carboxamide (45).** Compound **45** was prepared according to general procedure A using **39** (0.207 g, 1.0 mmol) as the starting material. Purified product **45** (yield: 0.099 g, 52%) was obtained as a white solid, mp 290-292 °C. <sup>1</sup>H NMR (400 MHz, DMSO-*d*<sub>6</sub>) δ 10.81 (s, 1H), 7.58 (s, 2H), 7.35 (t, *J* = 4.8 Hz, 1H), 7.01 (d, *J* = 4.9 Hz, 2H), 4.68 (s, 2H). <sup>13</sup>C NMR (100 MHz; DMSO-*d*<sub>6</sub>): δ 165.75, 164.84, 141.71, 128.08, 124.02, 123.47, 122.20, 118.34, 67.15. HRMS (*m/z*): [M + H]<sup>+</sup> calcd for C<sub>9</sub>H<sub>9</sub>N<sub>2</sub>O<sub>3</sub>, 193.0608; found: 193.0582.

**3-Oxo-2-phenyl-3,4-dihydro-2H-benzo[*b*][1,4]oxazine-8-carboxamide (46).** Compound **46** was prepared according to general procedure A using **40** (0.283 g, 1.0 mmol) as the starting material. Purified product **46** (yield: 0.097 g, 52%) was obtained as a white solid, mp 259-261 °C. <sup>1</sup>H NMR (400 MHz, DMSO-*d*<sub>6</sub>) δ 11.11 (s, 1H), 7.63 (br, 1H), 7.56 (br, 1H), 7.48 – 7.32 (m, 6H), 7.07 – 7.00 (m, 2H), 5.93 (s, 1H). HRMS (*m/z*): [M + H]<sup>+</sup> calcd for C<sub>15</sub>H<sub>13</sub>N<sub>2</sub>O<sub>3</sub>, 269.0921; found: 269.0894.

**2-(4-Methoxyphenyl)-3-oxo-3,4-dihydro-2H-benzo[*b*][1,4]oxazine-8-carboxamide (47).**

Compound **47** was prepared according to general procedure A using **41** (0.313 g, 1.0 mmol) as the starting material. Purified product **47** (yield: 0.116 g, 39%) was obtained as a white solid, mp 258-260 °C. <sup>1</sup>H NMR (400 MHz, DMSO-*d*<sub>6</sub>) δ 11.10 (s, 1H), 7.60 (br, 1H), 7.51 (br, 1H), 7.39

(dd,  $J = 7.0$  Hz, 1.7 Hz, 1H), 7.34 (d,  $J = 8.6$  Hz, 2H), 7.10 – 6.98 (m, 2H), 6.93 (d,  $J = 8.4$  Hz, 2H), 5.86 (s, 1H), 3.74 (s, 3H). HRMS ( $m/z$ ):  $[M + H]^+$  calcd for  $C_{16}H_{15}N_2O_4$ , 299.1026; found: 299.1004.

**2-(4-Bromophenyl)-3-oxo-3,4-dihydro-2H-benzo[*b*][1,4]oxazine-8-carboxamide (48).**

Compound **48** was prepared according to general procedure A using **42** (0.362 g, 1.0 mmol) as the starting material. Purified product **48** (yield: 0.104 g, 30%) was obtained as a white solid, mp 255-258 °C.  $^1H$  NMR (400 MHz, DMSO- $d_6$ )  $\delta$  11.13 (s, 1H), 7.70 – 7.49 (m, 4H), 7.46 – 7.29 (m, 3H), 7.04 (d,  $J = 5.1$  Hz, 2H), 5.92 (s, 1H). HRMS ( $m/z$ ):  $[M + H]^+$  calcd for  $C_{15}H_{12}^{79}BrN_2O_3$ , 347.0026; found: 347.0007 and calcd for  $C_{15}H_{12}^{81}BrN_2O_3$ , 349.0005; found: 349.0025.

**(Z)-2-(4-Hydroxybenzylidene)-3-oxo-3,4-dihydro-2H-benzo[*b*][1,4]oxazine-8-carboxamide (49).**

Compound **49** was prepared according to the reported procedure with modifications [28]. Compound **45** (0.192 g, 1.0 mmol) and 4-hydroxybenzaldehyde (0.183 g, 1.5 mmol) were added to a flask containing a 50:50 mixture of triethyl amine and acetic anhydride (10 mL:10 mL). The mixture was then refluxed for a period of 12 h and purified using preparative TLC to yield **49** (yield: 0.027 g, 8%) as a pale green solid, mp >310 °C.  $^1H$  NMR (400 MHz, DMSO- $d_6$ )  $\delta$  11.07 (s, 1H), 9.81 (s, 1H), 7.94 (s, 1H), 7.83 (d,  $J = 8.5$  Hz, 3H), 7.06 – 7.00 (m, 3H), 6.80 (d,  $J = 8.6$  Hz, 2H), 6.72 (s, 1H).  $^{13}C$  NMR (100 MHz; DMSO- $d_6$ ):  $\delta$  167.58, 157.97, 156.69, 138.97, 137.99, 132.16, 126.19, 125.49, 124.17, 122.90, 122.40, 116.65, 115.65, 112.13. HRMS ( $m/z$ ):  $[M + H]^+$  calcd for  $C_{16}H_{13}N_2O_4$ , 297.0870; found: 297.0850.

**(Z)-2-(4-Carboxybenzylidene)-3-oxo-3,4-dihydro-2H-benzo[*b*][1,4]oxazine-8-carboxamide (50).**

Compound **50** was obtained according to the procedure used for the preparation of compound **49**. Compound **45** (0.192 g, 1.0 mmol) and 4-carboxybenzaldehyde (0.225 g, 1.5

mmol) were employed to generate target compound **50** (yield: 0.031 g, 10%) as a dark yellow solid, mp >310 °C. <sup>1</sup>H NMR (400 MHz, DMSO-*d*<sub>6</sub>) δ 11.43 (s, 1H), 11.36 (s, 1H), 8.25 (d, *J* = 8.5 Hz, 1H), 7.98 – 7.91 (m, 4H), 7.81 (d, *J* = 8.3 Hz, 1H), 7.14 – 7.11 (m, 3H), 6.90 (s, 1H). <sup>13</sup>C NMR (100 MHz; DMSO-*d*<sub>6</sub>): δ 164.36, 162.87, 161.89, 154.68, 152.75, 144.14, 140.80, 139.02, 131.94, 130.64, 130.55, 127.34, 125.93, 116.22, 116.01. HRMS (*m/z*): [M + H]<sup>+</sup> calcd for C<sub>17</sub>H<sub>13</sub>N<sub>2</sub>O<sub>5</sub>, 325.2995; found: 325.3010.

### PARP1 enzyme assays and isoform profiling

Inhibitory activity against PARP1 was evaluated by *in vitro* PARP1 enzyme assay using the PARP Universal Chemiluminescent Assay Kit (Trevigen, Inc. Gaithersburg, MD) as described previously [9,15]. Compounds that showed more than 50% PARP1 inhibition at respective concentrations were further evaluated to obtain IC<sub>50</sub> values. The IC<sub>50</sub> values were determined from dose-response curves, which were plotted with absorbance against log of the concentrations (five concentration points for each compound), and obtained using regression wizard from Sigma Plot, version 10.0 (San Jose, CA).

The PARP1 inhibitory assays for compounds **49** and **50** were performed at BPS Bioscience using the BPS PARP1 Chemiluminescent Activity Assay Kit (Catalog #80551) using recently reported protocol [9]. Dose-response curves are depicted in supporting information Figures S3 and S4. The reported data, mean ± standard deviation (SD), are the averages from at least two independent dose-response curves, each carried out in triplicate. PARP-isoform screening for analogue **49** was performed at BPS Bioscience using the Chemiluminescent Activity Assay Kit (PARP2, catalog # 80502, PARP3, catalog # 80503, TNKS1, catalog #

80504, TNKS2, catalog # 80505, PARP8, catalog # 79076, PARP10, catalog # 80510 and PARP14, catalog # 80513) [9].

### **Conflicts of interest**

TTT is a co-founder of Hysplex, LLC, with interests in PARP inhibitor development. The other authors declare no competing financial interest.

**Funding:** This project was supported by the Department of Pharmaceutical Sciences of St. John's University; St. John's University Seed Grant No. 579-1110; and in part by the National Institute of General Medical Sciences (SC3GM131971) to T.T.T.

### **Acknowledgment**

We are grateful to Dr. Leonard Barasa (St. John's University) for his help during LC-MS analysis. We thank Dr. Suman Pathi for helpful discussions. We thank Dr. Brandon Fowler from the Department of Chemistry, Columbia University for his assistance in obtaining HR-MS data.

### **References**

- [1] M.F. Langelier, J.M. Pascal, PARP-1 mechanism for coupling DNA damage detection to poly(ADP-ribose) synthesis, *Curr. Opin. Struct. Biol.* 23(1) (2013) 134-143. DOI: 10.1016/j.sbi.2013.01.003.
- [2] K.W. Pratz, M.A. Rudek, I. Gojo, M.R. Litzow, M.A. McDevitt, J. Ji, L.M. Karnitz, J.G. Herman, R.J. Kinders, B.D. Smith, S.D. Gore, H.E. Carraway, M.M. Showel, D.E. Gladstone, M.J. Levis, H.L. Tsai, G. Rosner, A. Chen, S.H. Kaufmann, J.E. Karp, A phase I study of topotecan, carboplatin and the PARP inhibitor veliparib in acute leukemias, aggressive myeloproliferative neoplasms, and chronic myelomonocytic leukemia, *Clin. Cancer Res.* 23(4)

(2017) 899-907. DOI: 10.1158/1078-0432.ccr-16-1274.

[3] A.E. Wahner Hendrickson, M.E. Menefee, L.C. Hartmann, H.J. Long, D.W. Northfelt, J.M. Reid, F. Boakye-Agyeman, O. Kayode, K.S. Flatten, M.I. Harrell, E.M. Swisher, G.G. Poirer, D. Satele, J. Allred, J.L. Lensing, A. Chen, J. Ji, Y. Zang, C. Erlichman, P. Haluska, S.H. Kaufmann, A phase I clinical trial of the poly(ADP-ribose) polymerase inhibitor veliparib and weekly topotecan in patients with solid tumors, *Clin. Cancer Res.* 24(4) (2018) 744-752. DOI: 10.1158/1078-0432.ccr-17-1590.

[4] H.E. Bryant, N. Schultz, H.D. Thomas, K.M. Parker, D. Flower, E. Lopez, S. Kyle, M. Meuth, N.J. Curtin, T. Helleday, Specific killing of BRCA2-deficient tumours with inhibitors of poly(ADP-ribose) polymerase, *Nature* 434(7035) (2005) 913-917. DOI: 10.1038/nature03443.

[5] H. Farmer, N. McCabe, C.J. Lord, A.N. Tutt, D.A. Johnson, T.B. Richardson, M. Santarosa, K.J. Dillon, I. Hickson, C. Knights, N.M. Martin, S.P. Jackson, G.C. Smith, A. Ashworth, Targeting the DNA repair defect in BRCA mutant cells as a therapeutic strategy, *Nature* 434(7035) (2005) 917-921. DOI: 10.1038/nature03445.

[6] E.M. Swisher, W. Sakai, B.Y. Karlan, K. Wurz, N. Urban, T. Taniguchi, Secondary BRCA1 mutations in BRCA1-mutated ovarian carcinomas with platinum resistance, *Cancer Res.* 68(8) (2008) 2581-2586. DOI: 10.1158/0008-5472.can-08-0088.

[7] T. Fojo, S. Bates, Mechanisms of resistance to PARP inhibitors-three and counting, *Cancer Discov.* 3(1) (2013) 20-23. DOI: 10.1158/2159-8290.cd-12-0514.

[8] T.K. Ricks, H.J. Chiu, G. Ison, G. Kim, A.E. McKee, P. Kluetz, R. Pazdur, Successes and

challenges of PARP inhibitors in cancer therapy, *Front. Oncol.* 5 (2015) 222. DOI: 10.3389/fonc.2015.00222.

[9] U.K. Velagapudi, M.F. Langelier, C. Delgado-Martin, M.E. Diolaiti, S. Bakker, A. Ashworth, B.A. Patel, X. Shao, J.M. Pascal, T.T. Talele, Design and synthesis of Poly(ADP-ribose) polymerase inhibitors: Impact of adenosine pocket-binding motif appendage to the 3-oxo-2,3-dihydrobenzofuran-7-carboxamide on potency and selectivity, *J. Med. Chem.* 62(11) (2019) 5330-5357. DOI: 10.1021/acs.jmedchem.8b01709.

[10] L. Zandarashvili, M.F. Langelier, U.K. Velagapudi, M.A. Hancock, J.D. Steffen, R. Billur, Z.M. Hannan, A.J. Wicks, D.B. Krastev, S.J. Pettitt, C.J. Lord, T.T. Talele, J.M. Pascal, B.E. Black, Structural basis for allosteric PARP-1 retention on DNA breaks, *Science (New York, N.Y.)* 368(6486) (2020) DOI: 10.1126/science.aax6367.

[11] S.L. Dixon, A.M. Smondryev, E.H. Knoll, S.N. Rao, D.E. Shaw, R.A. Friesner, PHASE: a new engine for pharmacophore perception, 3D QSAR model development, and 3D database screening: 1. Methodology and preliminary results, *J. Comput. Aided Mol. Des.* 20(10-11) (2006) 647-671. DOI: 10.1007/s10822-006-9087-6.

[12] P. Jones, S. Altamura, J. Boueres, F. Ferrigno, M. Fonsi, C. Giomini, S. Lamartina, E. Monteagudo, J.M. Ontoria, M.V. Orsale, M.C. Palumbi, S. Pesci, G. Roscilli, R. Scarpelli, C. Schultz-Fademrecht, C. Toniatti, M. Rowley, Discovery of 2-{4-[(3S)-piperidin-3-yl]phenyl}-2H-indazole-7-carboxamide (MK-4827): a novel oral poly(ADP-ribose)polymerase (PARP) inhibitor efficacious in BRCA-1 and -2 mutant tumors, *J. Med. Chem.* 52(22) (2009) 7170-7185. DOI: 10.1021/jm901188v.

- [13] D.V. Ferraris, Evolution of poly(ADP-ribose) polymerase-1 (PARP-1) inhibitors. From concept to clinic, *J. Med. Chem.* 53(12) (2010) 4561-4584. DOI: 10.1021/jm100012m.
- [14] S.S. Kulkarni, S. Singh, J.R. Shah, W.K. Low, T.T. Talele, Synthesis and SAR optimization of quinazolin-4(3H)-ones as poly(ADP-ribose)polymerase-1 inhibitors, *Eur. J. Med. Chem.* 50 (2012) 264-273. DOI: 10.1016/j.ejmech.2012.02.001.
- [15] M.R. Patel, A. Bhatt, J.D. Steffen, A. Chergui, J. Murai, Y. Pommier, J.M. Pascal, L.D. Trombetta, F.R. Fronczek, T.T. Talele, Discovery and structure-activity relationship of novel 2,3-dihydrobenzofuran-7-carboxamide and 2,3-dihydrobenzofuran-3(2H)-one-7-carboxamide derivatives as poly(ADP-ribose)polymerase-1 inhibitors, *J. Med. Chem.* 57(13) (2014) 5579-5601. DOI: 10.1021/jm5002502.
- [16] B. Takahashi, H. Funami, T. Iwaki, H. Maruoka, M. Shibata, M. Koyama, A. Nagahira, Y. Kamiide, S. Kanki, Y. Igawa, T. Muto, Orally active ghrelin receptor inverse agonists and their actions on a rat obesity model, *Bioorg. Med. Chem.* 23(15) (2015) 4792-4803. DOI: 10.1016/j.bmc.2015.05.047.
- [17] W. Adam, E.M. Peters, K. Peters, H. Platsch, E. Schmidt, H.G. Von Schnering, K. Takayama, Synthesis, thermal stability, and chemiluminescence properties of the dioxetanes derived from 1,4-dioxins, *J. Org. Chem.* 49(21) (1984) 3920-3928. DOI: 10.1021/jo00195a008.
- [18] C. Rajitha, P.K. Dubey, V. Sunku, V.R. Veeramaneni, M. Pal,  $H_3PO_4/(CF_3CO)_2O$  mediated acylation followed by Hurd–Mori reaction: Synthesis of novel 1,2,3-thiadiazol derivatives, *J. Het. Chem.* 50(3) (2013) 630-637. DOI: doi:10.1002/jhet.1625.

- [19] T.M. Kuroita, N.; Sano, M.; Kanzaki, K.; Inaba, K.; Kawakita, T., Benzoxazines. II. Synthesis, conformational analysis, and structure--activity relationships of 3,4-dihydro-2H-1,4-benzoxazine-8-carboxamide derivatives as potent and long-acting serotonin-3 (5-HT<sub>3</sub>) receptor antagonists, *Chem. Pharm. Bull.* 44(11) (1996) 2051-2060. DOI: 10.1248/cpb.44.2051.
- [20] R.J. Griffin, A.H. Calvert, N.J. Curtin, D.R. Newell, B.T. Golding, Preparation of benzamide analogs as poly(ADP-ribose) polymerase inhibitors. *PCT Int. Appl.* 1995, A1 1995091, pp 79.
- [21] J.C. Ame, V. Rolli, V. Schreiber, C. Niedergang, F. Apiou, P. Decker, S. Muller, T. Hoger, J. Menissier-de Murcia, G. de Murcia, PARP-2, A novel mammalian DNA damage-dependent poly(ADP-ribose) polymerase, *J. Biol. Chem.* 274(25) (1999) 17860-17868. DOI: 10.1074/jbc.274.25.17860.
- [22] J.M. Rodriguez-Vargas, L. Nguekeu-Zebaze, F. Dantzer, PARP3 comes to light as a prime target in cancer therapy, *Cell cycle (Georgetown, Tex.)* 18(12) (2019) 1295-1301. DOI: 10.1080/15384101.2019.1617454.
- [23] A. Mizutani, Y. Yashiroda, Y. Muramatsu, H. Yoshida, T. Chikada, T. Tsumura, M. Okue, F. Shirai, T. Fukami, M. Yoshida, H. Seimiya, RK-287107, a potent and specific tankyrase inhibitor, blocks colorectal cancer cell growth in a preclinical model, *Cancer Sci.* 109(12) (2018) 4003-4014. DOI: 10.1111/cas.13805.
- [24] M.T. Rubino, D. Maggi, A. Laghezza, F. Liodice, P. Tortorella, Identification of novel matrix metalloproteinase inhibitors by screening of phenol fragments library, *Archiv. der Pharmazie* 344(9) (2011) 557-563. DOI:10.1002/ardp.201000350.

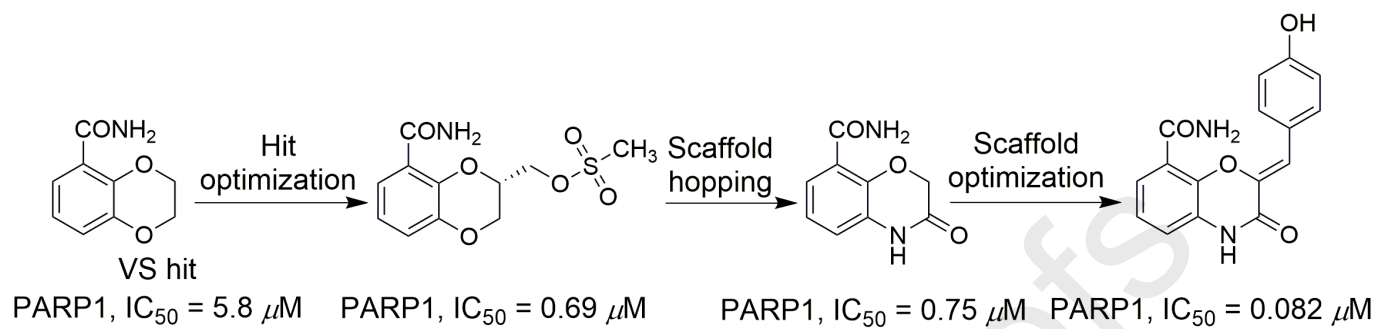
- [25] T. Heinrich, H. Böttcher, H. Prücher, R. Gottschlich, K.-A. Ackermann, C. van Amsterdam, 1-(1-Phenethylpiperidin-4-yl)-1-phenylethanols as potent and highly selective 5-HT<sub>2A</sub> antagonists, *ChemMedChem* 1(2) (2006) 245-255. DOI: 10.1002/cmdc.200500023.
- [26] C. Bolchi, L. Fumagalli, B. Moroni, M. Pallavicini, E. Valoti, A short entry to enantiopure 2-substituted 1,4-benzodioxanes by efficient resolution methods, *Tetrahedron: Asymmetry* 14(23) (2003) 3779-3785. DOI: 10.1016/j.tetasy.2003.09.012.
- [27] L. Costantino, F. Gandolfi, C. Sorbi, S. Franchini, O. Prezzavento, F. Vittorio, G. Ronsisvalle, A. Leonardi, E. Poggesi, L. Brasili, Synthesis and structure-activity relationships of 1-aralkyl-4-benzylpiperidine and 1-aralkyl-4-benzylpiperazine derivatives as potent sigma ligands, *J. Med. Chem.* 48(1) (2005) 266-273. DOI: 10.1021/jm049433t.
- [28] T. Honda, T. Terao, H. Aono, M. Ban, Synthesis of novel 1,4-benzoxazin-3-one derivatives as inhibitors against tyrosine kinases, *Bioorg. Med. Chem.* 17(2) (2009) 699-708. DOI: 10.1016/j.bmc.2008.11.060.

### Conflicts of interest

TTT is a co-founder of Hysplex, LLC, with interests in PARP inhibitor development. The other authors declare no competing financial interest.

### Highlights

- Structure- and pharmacophore-based virtual screening led to 2,3-dihydrobenzo[*b*][1,4]dioxine-5-carboxamide (compound **4**, IC<sub>50</sub> = 5.8 μM).
- Compound **4** was optimized via analogue synthesis and scaffold hopping.
- Series of regioisomeric pairs were assigned using HMBC NMR technique.
- (*Z*)-2-(4-hydroxybenzylidene)-3-oxo-3,4-dihydro-2*H*-benzo[*b*][1,4]oxazine-8-carboxamide (**49**, IC<sub>50</sub> = 0.082 μM) was identified as the most potent inhibitor.
- Docking model of **49**-PARP1 complex will facilitate future optimization.



Journal Pre-proofs